Chem Soc Rev

REVIEW ARTICLE

View Article Online
View Journal | View Issue

Cite this: *Chem. Soc. Rev.*, 2020, **49**, 4254

3d metallaelectrocatalysis for resource economical syntheses

Parthasarathy Gandeepan, †[ab] Lars H. Finger, †[a] Tjark H. Meyer [a] and Lutz Ackermann *[acd]

Resource economy constitutes one of the key challenges for researchers and practitioners in academia and industries, in terms of rising demand for sustainable and green synthetic methodology. To achieve ideal levels of resource economy in molecular syntheses, novel avenues are required, which include, but are not limited to the use of naturally abundant, renewable feedstocks, solvents, metal catalysts, energy, and redox reagents. In this context, electrosyntheses create the unique possibility to replace stoichiometric amounts of oxidizing or reducing reagents as well as electron transfer events by electric current. Particularly, the merger of Earth-abundant 3d metal catalysis and electrooxidation has recently been recognized as an increasingly viable strategy to forge challenging C–C and C–heteroatom bonds for complex organic molecules in a sustainable fashion under mild reaction conditions. In this review, we highlight the key developments in 3d metallaelectrocatalysis in the context of resource economy in molecular syntheses until February 2020.

Received 20th February 2020

DOI: 10.1039/d0cs00149j

rsc.li/chem-soc-rev

[a] *Institut für Organische und Biomolekulare Chemie, Georg-August-Universität Göttingen, Tammannstraße 2, 37077 Göttingen, Germany. E-mail: Lutz.Ackermann@chemie.uni-goettingen.de; Web: http://www.ackermann.chemie.uni-goettingen.de/index.html*

[b] *Department of Chemistry, Indian Institute of Technology Tirupati, Tirupati, Andhra Pradesh 517506, India*

[c] *Woehler Research Institute for Sustainable Chemistry (WISCh), Georg-August-Universität Göttingen, Tammannstraße 2, 37077 Göttingen, Germany*

[d] *Department of Chemistry, University of Pavia, Viale Taramelli 10, 27100 Pavia, Italy*

† These authors contributed equally to this work.

Parthasarathy Gandeepan

Parthasarathy Gandeepan has been Assistant Professor in the Department of Chemistry at the Indian Institute of Technology Tirupati since December 2019. He studied BSc (Chemistry) and MSc (Organic Chemistry) at the University of Madras and obtained his PhD (Chemistry) with Chien-Hong Cheng at the National Tsing Hua University, Taiwan. He did postdoctoral works with Chien-Hong Cheng (NTHU, Taiwan), Lutz Ackermann (University of Göttingen, Germany), and Beatrice Collins (University of Bristol, UK) before starting his independent research career. His research interests include transition metal-catalyzed organic transformations, photoredox catalysis, and sustainable methodology developments for organic synthesis. He is teaching Organic Chemistry courses to graduate and postgraduate students.

Lars H. Finger

Lars Finger studied chemistry at the Philipps-University Marburg and spent one semester at the Heriot-Watt University Edinburgh. He received his PhD from the PU Marburg in 2016 under the supervision of Prof. Jörg Sundermeyer, working on organic salts with azolate and chalcogenolate anions for electrochemical applications. In 2017, Lars joined the group of Prof. Lutz Ackermann as a post-doctoral fellow focusing on C–H activation by metallaelectrocatalysis.

1. Introduction

In the last few decades, significant attention has been paid to the development of sustainable strategies for molecular assembly in terms of both economic and environmental benefits.[1] In 1991, Trost proposed the concept of atom economy and highlighted the value of transition metal catalysis towards this goal.[2,3] Later, Anastas and Warner introduced the twelve principles of green chemistry in 1998 to provide guidelines for minimizing the environmental footprint of chemical syntheses.[4] Further, the principles of step economy[5] and redox economy have been put forward.[6,7] In contrast, resource economy aims to provide a basis for designing fully sustainable methodologies of molecular syntheses.[8] These principles are reflected by the development of the corresponding techniques (Fig. 1a). Considering the transformation of two organic reactants with the corresponding reactive groups, the cross-coupling catalysis was developed. C–H activation allowed the use of even less functionalized starting materials.[9–18] Metallaphotocatalysis offers the potential to drive catalytic processes from solar energy.[19–21] This is finally accomplished with metallaelectrocatalysis, which in addition has recently gained momentum by outstanding cooperativity effects with base metal catalysts. In this regard, metallaelectrocatalysis has emerged as a potent strategy to achieve selective chemical syntheses (Fig. 1b). In this review, we focus on the recent developments to achieve improved resource economy in molecular syntheses by combining Earth-abundant 3d metal catalysis and electrooxidation towards ideal resource economy until February 2020.

2. Resource economy in organic syntheses

The economy of Synthesis

Atom economy: Maximizing the number of atoms of raw materials that are incorporated in the desired products

Step economy: Reducing the number of reaction steps for efficient chemical syntheses

Redox economy: Minimization of redox manipulations in order to achieve an ideally isohypsic synthesis

Resource economy: Minimizing the overall footprint of chemical transformations as to the complete life cycle analysis, including, but not being limited to the use of naturally abundant or renewable feedstocks, solvents, metal catalysts, energy, and redox reagents

Organic syntheses based on multi-step functional group transformations should ideally be avoided because of their low atom-and step-economy. In contrast, transition metal-catalyzed C–H activation has been established as a potent tool to achieve high levels of atom- and step-economy by employing non-functionalized starting materials.[22–33] Despite significant advances, precious transition metal catalysts, such as palladium, rhodium, ruthenium, and iridium, are predominantly required for achieving high efficiencies. In stark contrast, recent developments in this rapidly evolving arena suggested the use of Earth-abundant 3d transition metal complexes as

Tjark H. Meyer

Tjark H. Meyer studied chemistry at the Georg-August-University Göttingen and obtained his MSc in 2016 under the supervision of Prof. L. Ackermann. During his studies he joined the group of Dr Stephen P. Thomas at the University of Edinburgh for a four-month research stay, and later, he performed an industrial placement at Bayer AG, Wuppertal. In 2017, he started his doctoral studies in the group of Prof. L. Ackermann. His current research is focused on synthetic organic electrochemistry, with a major interest on the merger of metal-catalysed C–H activation and electrocatalysis.

Lutz Ackermann

Lutz Ackermann studied chemistry at the Christian-Albrechts University Kiel and obtained his PhD in 2001 with Alois Fürstner at the MPI für Kohlenforschung in Mülheim/Ruhr. He was a postdoctoral fellow with Robert G. Bergman (UC Berkeley) before initiating his independent research in 2003 at the Ludwig-Maximilians University München, supported within the Emmy Noether Program of the DFG. In 2007, he became full professor at the Georg-August University Göttingen, where he served as the Dean of Research and Dean of Chemistry as well as the director of the Wöhler Research Institute for Sustainable Chemistry (WISCh). The development of novel concepts for homogeneous catalysis and their applications to sustainable organic synthesis, late-stage peptide diversification, and molecular imaging are among his main current research interests.

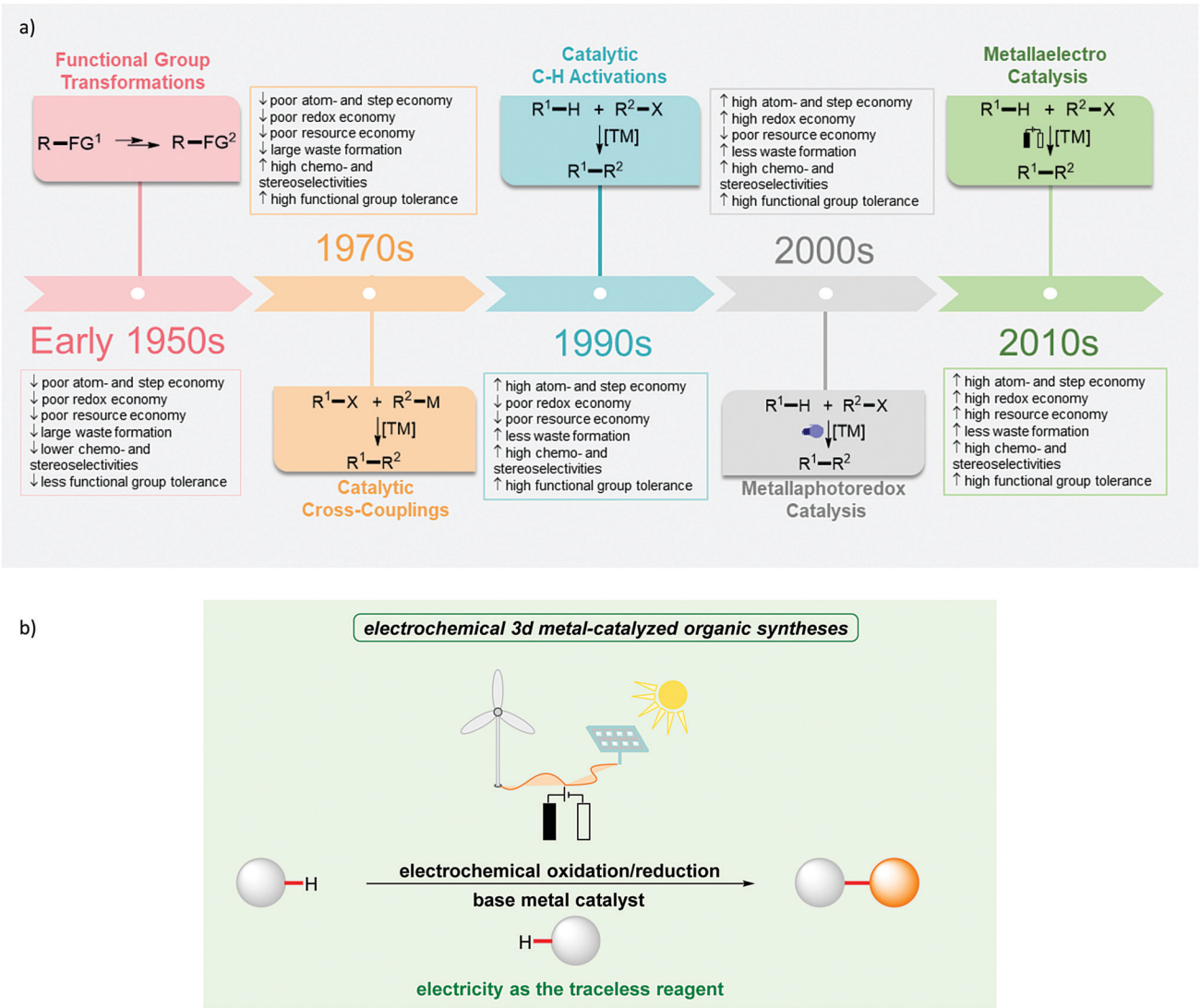

Fig. 1 General overview for enhancing the economy of organic syntheses. (a) General paradigm shift in catalytic organic syntheses. (b) Achieving resource economy by electrochemical 3d metal-catalyzed organic transformations.

catalysts in C–H activation reactions.[34,35] However, oxidative transition metal-catalyzed transformations usually demand stoichiometric amounts of toxic and expensive metals oxidants. This requirement compromises the overall sustainable nature of the C–H activation strategy by generating often toxic metal wastes, high production costs, and overall poor resource economy.

Considering its natural abundance, the use of molecular oxygen as the terminal oxidant in transition metal-oxidase catalysis continues to be of topical interest.[36–38] Despite the improved sustainability and resource economy, the use of oxygen is on the one hand limited by its fixed oxidation potential. On the other hand, and more importantly, major safety hazards in view of flammable reaction media in large scale syntheses need to be addressed, rendering this approach challenging particularly for scale-up.[39]

As a consequence, in recent years, photoredox catalysis has emerged as a strategy to affect redox processes in transition metal catalysis in a mild and selective manner.[40–45] These transformations are mostly based on noble iridium or ruthenium complexes as the photoredox catalyst (PC) to convert light into chemical energy. It is noteworthy that each PC offers only a unique fixed redox potential and therefore the use and synthesis of specifically tailored PCs are essential to realize the desired redox transformation (Fig. 2, top). The synthetic modification of PCs to adjust the redox potential typically demands labor- and cost-intensive multistep transformations. Though the power of photoredox catalysis has evidently been demonstrated for transition metal catalysis,[46] the quantum yields of these transformations are typically low when employing visible light, and natural sunlight can normally not be used, because of the narrow absorption range of the PCs. In contrast, high power LEDs or Kessil LED lights are often necessary for satisfactory efficacy.

In sharp contrast, the direct use of electric current for the development of new redox strategies sets the stage for the

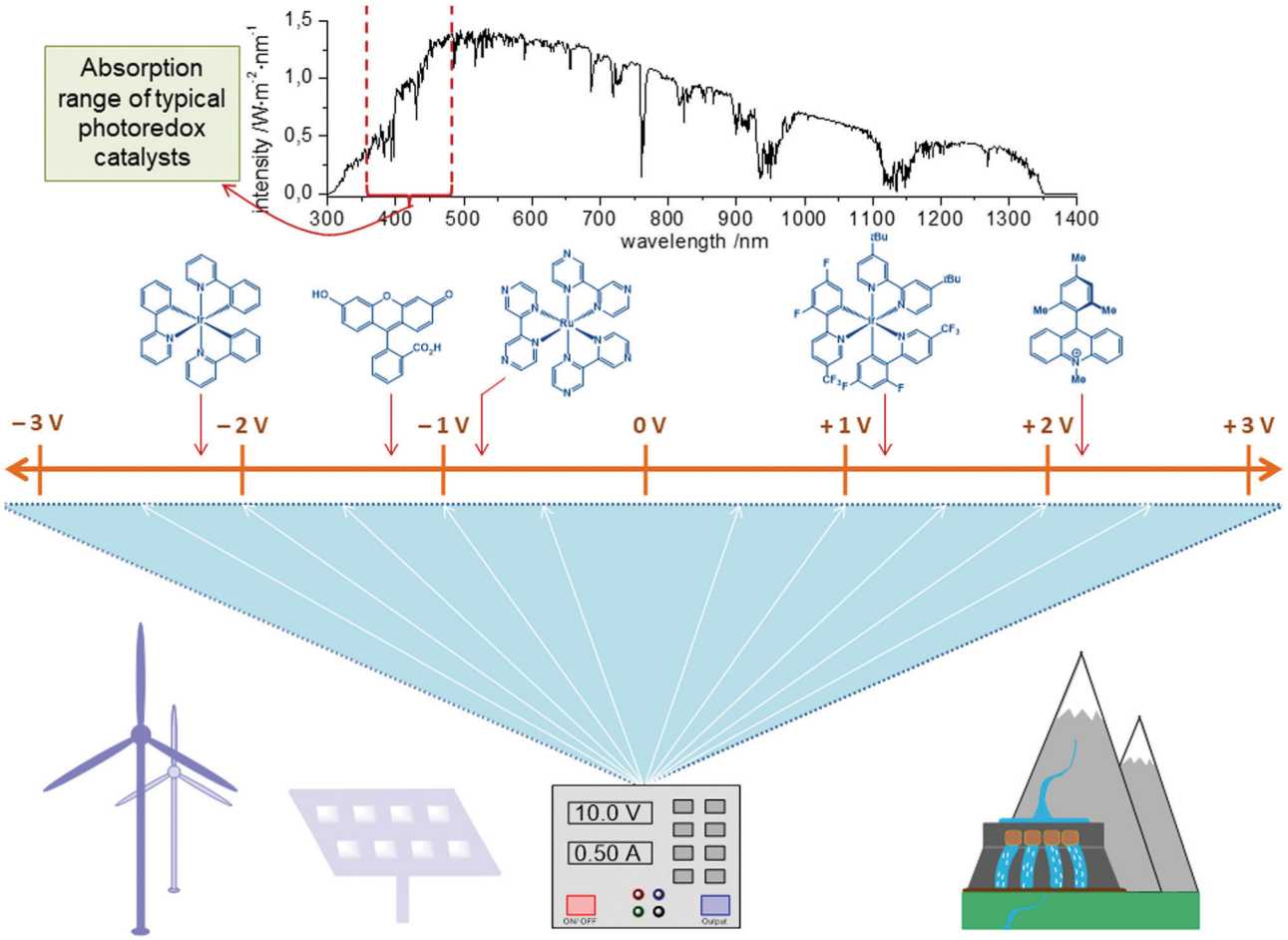

Fig. 2 While photo catalysts offer only selected, fixed potentials and can use only a very limited part of the solar spectrum, a potentiostat gives access to the complete potential range with high precision and can be powered exclusively by sustainable energy sources.

efficient utilization of available energy sources, such as solar or wind power. The infinitely variable redox potential is easily set at the flick of a switch (Fig. 2, bottom). In electrocatalysis, electrons serve as an inherently clean redox reagent to drive the redox process and avoid stoichiometric reagent waste. The controllable redox potential generally allows for improved functional group tolerance and high levels of chemo- and regio-selectivity. Realizing the great potential for resource economy, several organic transformations have been developed, which merge traditional oxidative transformations with electrolysis, which has been reviewed elsewhere.[47–50]

The full potential of dual electron catalysis and transition metal catalysis – coined metallaelectrocatalysis – to enable efficient organic transformations has only recently been recognized.[51–53] Until very recently, the use of Earth-abundant 3d metal catalysts in metallaelectrocatalysis for otherwise inert bond activation had proven elusive.[54] In addition to their Earth-abundance, 3d metals are cost-effective and generally less toxic in comparison with their noble 4d and 5d homolouges.[55] The outstanding capacity for resource economy has made base metal-catalyzed metallaelectrocatalysis an invaluable platform for organic synthesis.[8,56]

3. Principles, tools, and design of metallaelectrocatalysis

3.1 History

The development of the voltaic pile by Alessandro Volta in Pavia as the first continuous source of electricity[57] set the stage for the development of a wealth of further inventions. Importantly it allowed Sir Michael Faraday to quantify electrochemical syntheses by his laws of electrolysis. He also noticed the formation of hydrocarbons during the electrolysis of dilute potassium acetate solution.[58] Hermann Kolbe, who was born and educated in Göttingen as a student of Friedrich Wöhler, then identified and isolated ethane, carbon dioxide, hydrogen and dimethyl ether as the products of the electrolysis of a series of carbonic acids.[59]

3.2 Tools, design and principles

When an electrode is immersed in a solution of a half-cell, the difference between the solution's and the electrode material's electrochemical potential leads to a charge separation at the electrode–electrolyte interface originating from the systems attempt to reach equilibrium. It is extremely challenging to

experimentally determine the value of this electrochemical potential difference. Two distinct half-cells will differ in the amount of charge that accumulates on the electrode surface. If these two half cells are connected, without allowing a flow of electric charge, this difference between the two equilibrium electrode potentials can be measured as an electric potential difference with a voltmeter. The standard hydrogen electrode (SHE) has been chosen as a reference system and its equilibrium electrode potential was defined as 0 V by convention. Therefore, by measuring any cell *versus* the SHE, the equilibrium electrode potential of the specific half-cell can be determined. The Nernst – eqn (I) relates the potential of a half-cell to the activity of the corresponding species of the redox couple: Instead of the activities, the respective concentrations are commonly used as an approximation. As soon as current flows and an electrochemical reaction occurs, the Nernst-Equation is no longer valid.

$$E = E^0 + \frac{R \cdot T}{n_e \cdot F} \ln \frac{a_{Ox}}{a_{Red}} \quad \text{(I)}$$

E^0 is the standard electrode potential, *i.e.*, the potential of the half-cell under standard conditions, R is the universal gas constant, T is the temperature in K, a_{Ox} and a_{Red} are the activities of the oxidized and reduced species, respectively.

An electrochemical cell consists of at least two electrodes in contact with the electrolyte. Electrons are transported in the electric connections of the electrodes and the circuit is closed by ion movement in the electric field developed between the electrodes in the electrolyte. Electrochemical cells can be divided into two subtypes with respect to their working principle. In a galvanic cell – the voltaic pile consists of several galvanic cells connected in series – electricity is generated until the components of the cell have reached chemical equilibrium. In contrast, in an electrolytic cell a chemical reaction is powered by electricity. In this case, substances are oxidized at a positively charged anode by transferring electrons to the electrode. Simultaneously, at the negatively charged cathode substances are reduced by accepting electrons from the electrode. The two most important characteristics of an electrolytic cell are the potential or voltage (U in Volt) and the current (I in Ampere). Considering a molecular approach, the potential can be viewed as the energy level of the electrons in the electrode. A highly negative value corresponds to a strongly reducing behavior, whereas a high positive value denotes a strong oxidative force. The current relates *via* Faraday's laws of electrolysis to the number of electrons, which are passed through the solution (eqn (II)).

$$n_e = \frac{I \cdot t}{F} \quad \text{(II)}$$

n_e is the number of electrons, I is the current in A, t is the time in seconds, F = 96485.33 C mol^{-1} is the Faraday constant. Note: $F = N_A \cdot e$ with N_A as the Avogadro constant and e the elementary charge.

The faradaic yield or often Faraday efficiency (FE) is the percentage value that specifies the ratio of Coulombs consumed in forming the chemical products to the total number of Coulombs passed through the cell. This is expressed in the following formula (eqn (III)):

$$FE = \frac{n_e \cdot n_{Prod} \cdot F}{Q_{tot}} \times 100 \quad \text{(III)}$$

n_e is the number of electrons added to or removed from one product molecule, n_{Prod} the amount of product in mol and Q_{tot} the total charge passed through the cell ($Q_{tot} = I \cdot t$) in Coulomb.

According to Ohm's law, the potential is proportional to the current with the resistance (R) being the constant of proportionality ($U = R \cdot I$). This implies that only one of these values can be preset in an experiment, while the second one will adapt according to the cell's resistance. The first option is to keep the current constant (CCE = constant current electrolysis). This results in a potential difference between the electrodes, which enables the charge to pass through the cell at this specific rate. This option is advantageous in terms of directly controlling the amount of charge accompanied by a simple setup. However, during an electrochemical synthesis, the potential will typically increase, while the reactants are consumed and the cell resistance rises. This may lead to undesired side reactions and will decrease the current efficiency towards high substrate conversions (Fig. 3a). Alternatively, a fixed potential can be applied (CPE = constant potential electrolysis), which results in an adapting current. This can allow more chemo-selective transformations with high current efficiency so that ideally only the desired transformation takes place. However, during the electrosynthesis the current decreases due to depletion of the reactants and accordingly the reaction slows down (Fig. 3b). Additionally, a CPE requires more sophisticated equipment. A reference electrode as a third electrode in the electrochemical cell is mandatory to reliably control the working electrode's potential. At the reference electrode no electrochemical reaction takes place and no electric current flows. If the potential of one electrode is measured *versus* the live counter electrode, an unknown overpotential (*vide infra*) arises. The reference electrode must be chosen according to the system at hand. For aqueous electrolyte mixtures, Hg/Hg_2Cl_2 (calomel) or Ag/AgCl reference electrodes are well suited. For short reaction times, these can usually be applied in organic reaction media as well. Several organic solvent-based Ag/Ag(I) reference electrodes have also been developed. For a first approximation, it can be sufficient to use an inert metal wire as a pseudo reference electrode.

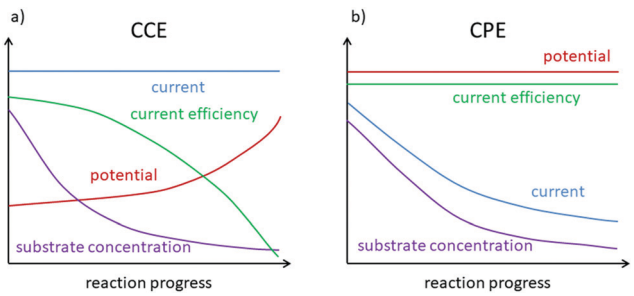

Fig. 3 Comparison of theoreatical reaction profiles for CCE and CPE.

It has to be taken into account, though, that an alteration of the metal surface or the solvent pH and composition may lead to a change of the inherent potential of the reference electrode in the electrolyte. This ultimately leads to a drift of the reference potential and reduces the accuracy with which the potential is kept constant.

The electrolyte in electrolytic cells mostly consists of a conducting agent dissolved in an organic solvent or aqueous media. Overall there are few limitations regarding the choice of solvents for electrosynthesis. However, in addition to the usual aspects of solvent selection for chemical reactions, such as polarity, boiling point, coordination behavior and solubility of reactants and reagents – to name a few – also the stability towards electrolysis and electro-generated reactive intermediates as well as the conductivity are of prime importance. Usually, conducting agents have to be employed to decrease the resistance of the electrolyte. The same restrictions as for the solvent apply. Most importantly, the electrolyte mixture should be electrochemically stable within the potential window that is needed for the desired transformation. Information regarding the stability of common electrolyte mixtures in terms of the applied potential can be found elsewhere.[60]

Electrolytic cells can be differentiated depending on whether a divided or undivided setup is employed (Fig. 4). In an undivided cell the electrodes are in the same compartment of the reaction vessel and all species in solution can diffuse freely between the electrodes. In contrast, in a divided cell the anode and cathode compartments are separated by a semi-permeable, often ion-selective membrane or a glass frit of very fine porosity. These barriers allow for the diffusion of small ions for the necessary charge transport but hinder the diffusion of larger molecules. Thereby, sensitive species reacting or being formed at the one electrode, are protected from the counter electrode itself and the majority of thus-formed by-products. The undivided cell setup comes in general at a lower price and is easily constructed from almost any reaction vessel in a synthetic lab.

Whereas the reaction between a chemical oxidant (or reductant)[61] and a substrate is usually a homogeneous process between two dissolved species, the electrooxidation of a substrate is always occurring at an electrode surface in a heterogeneous surface process. This leads to a series of effects, which result in an overpotential for the respective redox event. The overpotential is the difference between the equilibrium redox potential (the potential difference *versus* the SHE without current flow) of the species to be oxidized and the actual potential at the electrode, at which the redox event takes place.

The kinetic barrier for the actual electron transfer step from the substrate to the electrode will be different from the barrier observed between two dissolved species. Depending on the electrode material and its interaction with the substrate species, an activation overpotential is observed.

The polarization of the electrode leads to the formation of an electrochemical double layer. At a positively charged anode anionic species will accumulate to achieve microscopic charge compensation. In order to react at the electrode surface, any species has to diffuse through the double layer, potentially rearrange its solvation and after the reaction diffuse back into the bulk solution. In addition, further chemical reaction steps prior to or after the electron transfer may have to be taken into account. All these subsequent steps determine the concentration of the active substrate species at the electrode surface and thereby lead to a concentration overpotential. The activation overpotential and concentration overpotential both increase with the current density at the electrode.

The resistance of the cell components – especially the electrode–electrolyte junctions – and of the electrolyte itself (Ohmic drop or IR drop) have to be taken into account likewise. The resistance can increase drastically, if a precipitate or gas bubbles form at the electrode and thereby decrease the active electrode surface.

However, in certain cases, the overpotential can also be exploited for the tailoring the reactions. For instance, platinum metal is characterized by a very low overpotential for the formation of hydrogen gas by proton reduction. Therefore, using a platinum cathode is effective in promoting hydrogen formation and suppressing other possibly undesired cathodic reductions. The use of platinum as the electrode material, albeit costly, takes a little toll on the resource economy as the electrode is reusable. However, nickel and iron both show low overpotentials for hydrogen formation as well and may be more resource economic alternatives, where possible.

A high overpotential can also be circumvented by using a mediator for indirect electrolysis of the substrate (Fig. 5). In direct electrolysis, the substrate is oxidized at the electrode surface.

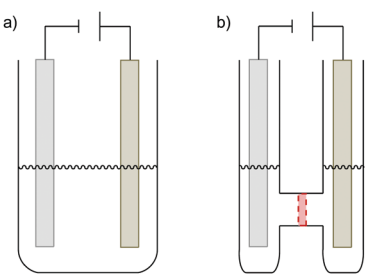

Fig. 4 (a) Undivided and (b) divided (H-type) electrochemical cell.

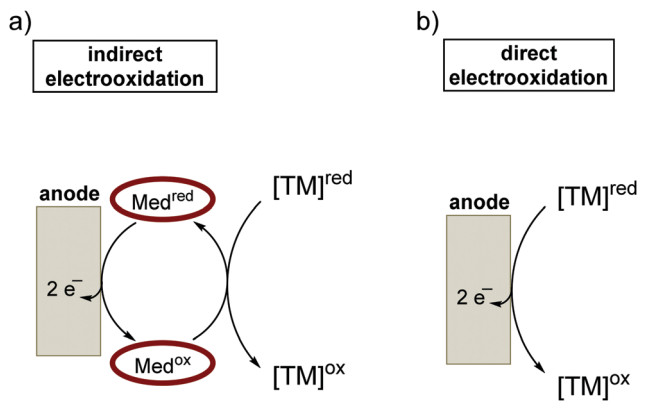

Fig. 5 Direct and indirect (mediated) electrolysis.

An indirect electrolysis[62] is characterized by the substrate being oxidized by a second dissolved species, which in turn is oxidized at the anodic surface. The redox mediator, which is usually employed in catalytic amounts, acts as an electron shuttle between the electrode and the substrate. This strategy may allow more selective transformations if the overpotential needed for direct electrolysis of the substrate is significantly higher than that for the oxidation of the redox mediator. In terms of resource economy, the use of a redox mediator is in principle unfavorable, as it decreases the atom economy. However, potential benefits like the decreased formation of side products and less energy consumption have to be carefully considered in the individual case.

4. Case studies of resource economical metallaelectrocatalysis

4.1 Case study I: oxidative difunctionalization of alkenes

Transition metal catalysis has the power to improve the control of the reaction chemo-selectivity and thus can expand reaction scope and synthetic utility. In this context, metallaelectrocatalysis provides an innovative platform to realize the oxidative difunctionalization of alkenes in a sustainable fashion.[63] The electrochemical approach offers an alternative approach to perform radical alkene functionalization in the absence of hazardous or expensive chemical oxidants.[64–73]

Although a few examples have been known since the 1990's for electrochemical organometallic difunctionalization of olefins, such as epoxidations by manganese salen complexes,[74,75] and dihydroxylations using osmium catalysts,[76,77] this area of research has gained significant momentum by the exciting work involving manganese-catalyzed diazidation of alkenes **1** as reported by Lin and coworkers in 2017 (Scheme 1).[78] Supported by mechanistic studies, a Mn(II)/Mn(III) redox cycle has been proposed for this electrochemical radical alkene difunctionalization (Scheme 1b). The mechanism involves the formation of a [Mn(II)]–N_3 coordination compound, which is oxidized to [Mn(III)]–N_3 and then transfers $\bullet N_3$ to the alkene, regenerating the [Mn(II)] species. In a second analogous sequence the product **2** is generated. The reaction proved compatible with terminal, 1,1- and 1,2-disubstituted, trisubstituted, and tetrasubstituted olefins to provide the desired 1,2-diazides **2** in high yields. The mild electrocatalytic reaction conditions offered high chemoselectivity and various synthetically meaningful functional groups, such as ester, alcohol, ketone, carboxylic acid, and amine, on the alkene moiety were well tolerated (Scheme 1c). The resource economy of the reaction is substantiated by the Earth-abundant manganese catalyst, a high faradaic efficiency (66–87%), high atom economy, and hydrogen and sodium acetate as benign by-products. In a related study, the authors also accomplished the dichlorination of alkenes **1** with $MgCl_2$ as the chlorine source under mild reaction conditions.[79] It is worth mentioning that the diazidation of alkenes **1** has subsequently also been realized under transition metal free reaction conditions using aminoxyl radical catalyst, CHAMPO.[80]

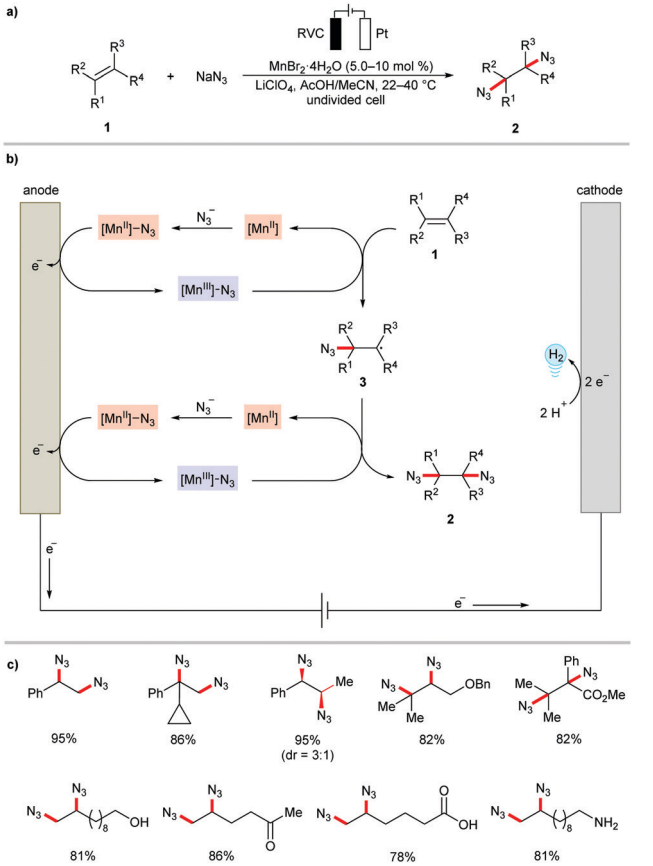

Scheme 1 Manganese-catalyzed electrochemical diazidation of alkenes **1**. RVC: reticulated vitreous carbon.

The versatile metallaelectrocatalysis was further applied to the heterodifunctionalization of alkenes **1** (Scheme 2).[81] Thus, the manganese-catalyzed electrochemical reaction conditions enabled the synthetically valuable chlorotrifluoromethylation of alkenes **1** using commercially available bench-stable $MgCl_2$, and CF_3SO_2Na (Langlois reagent) as the Cl and CF_3 source, respectively. The proposed catalytic cycle involves the anodic generation of the $\bullet CF_3$ radical and [Mn(III)]–Cl (Scheme 2b). Subsequently, the $\bullet CF_3$ attacks the alkene to generate a transient carbon-centered radical species **5**, which is trapped within a radical coupling with [Mn(III)]–Cl to provide the desired chlorotrifluoromethylation product **4**. The electrocatalytic conditions conveniently transformed diversely substituted alkenyl substrates **1** into the desired products **4** at ambient reaction temperature (Scheme 2c). Interestingly, the difunctionalization of 1,6-enyne substrates **6** afforded chlorotrifluoromethylated pyrrolidines under only slightly modified reaction conditions.[82] Here, the presence of the bidentate ligand 2,2′-bipyridine (bpy) significantly enhanced the stereo control of the alkenyl group in the pyrrolidine products **7** (Scheme 3).

Most recently, the Lin group has further showcased the application of anodically coupled heterodifunctionalization to the chloroalkylation of alkenes **1** (Scheme 4).[83] The protocol allowed for the simultaneous construction of vicinal C–C and C–Cl bonds under mild conditions in the presence of catalytic

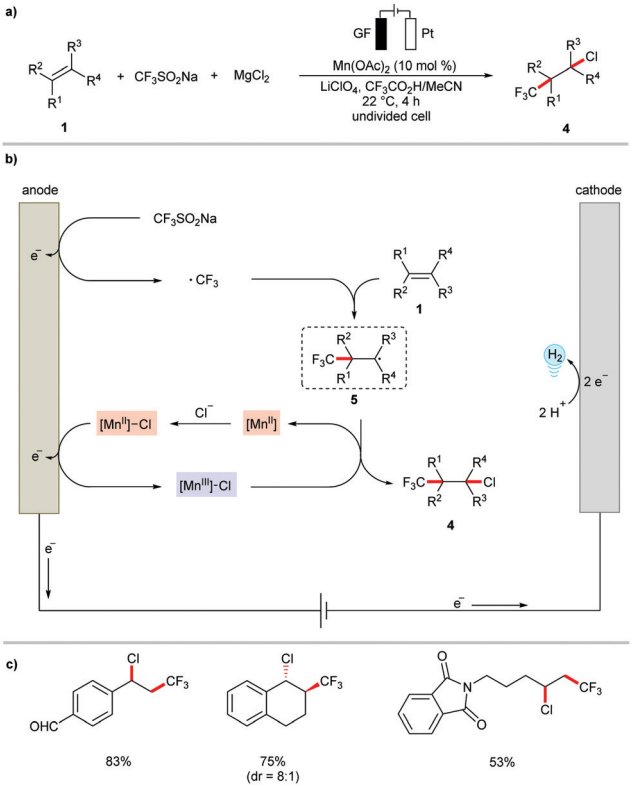

Scheme 2 Manganese-catalyzed electrochemical chlorotrifluoromethylation of alkenes **1**. GF: Graphite felt.

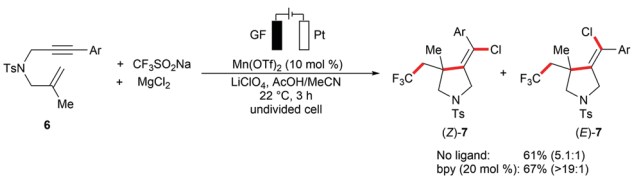

Scheme 3 Electrocatalytic synthesis of chlorotrifluoromethylated pyrrolidines **7**.

amounts of $Mn(OTf)_2$. Here, malononitriles **8** and cyanoacetates were employed as alkyl substrates and NaCl as the chlorine source. A plausible catalytic cycle was proposed to involve a parallel, manganaelectro-catalyzed generation of alkyl and chlorine radicals followed by selective addition to olefins (Scheme 4b).

4.2 Case study II: cross-coupling reactions

During the past decades, palladium-catalyzed cross-couplings have emerged as promising and widely used reactions to forge C–C and C–heteroatom bonds in drug molecules and functional materials.[84–87] Particularly, C–N forming reactions are often required in API syntheses.[88–90] In view of the high cost and low natural occurrence of palladium, significant efforts have been devoted to enable these cross-coupling reactions using Earth-abundant nickel catalysts. However, these methods often demand drastic reaction conditions, including high reaction temperatures, strong bases, and air-sensitive nickel(0)

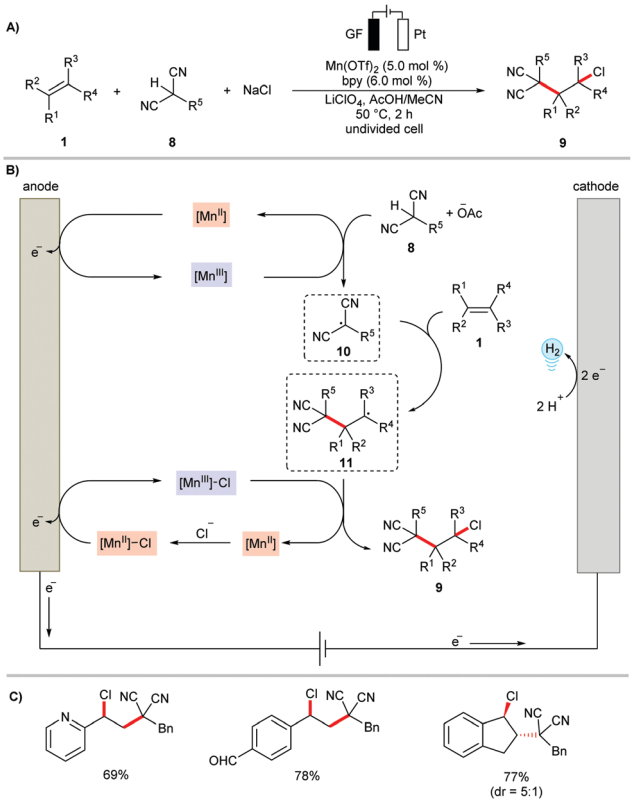

Scheme 4 Manganese-catalyzed chloroalkylation of alkenes **1**.

pre-catalysts,[91–95] which limits their application to late-stage modifications.[96]

In this context, the Baran group recently reported an effective method to construct C–N bonds by cross-coupling of aryl bromides **12** with alkyl amines **13** under electrochemical nickel[97] catalysis (Scheme 5).[98] The reaction was performed in an undivided cell in the presence of catalytic amounts of air-stable nickel complex $NiBr_2$·glyme and di-*t*Bubpy as the ligand. A variety of (hetero)aryl bromides **12** were efficiently transformed into the corresponding (hetero)arylamines **14** in

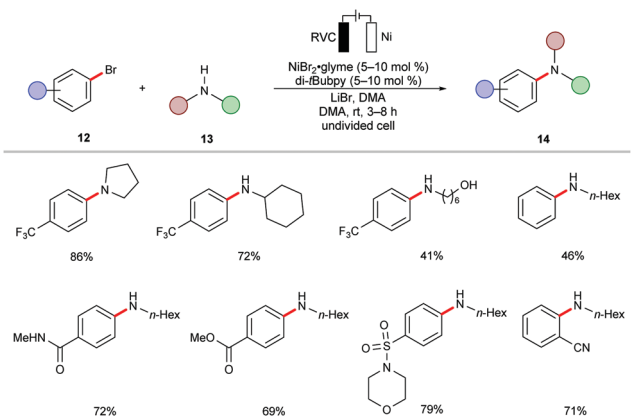

Scheme 5 Electrochemical nickel-catalyzed amination of aryl bromides **12**.

high yields. Sensitive functional groups, including cyano, ester, hydroxyl, amide and sulfonamide, were thereby well tolerated.

In subsequent efforts, the same group further expanded the scope of viable amines to include amino acid esters **15** and small oligopeptides under slightly adjusted reaction conditions (Scheme 6a).[99] The application of the nickel-catalyzed electrochemical C–H amination protocol was successfully employed as a key step in the total synthesis of Teleocidins B-1–B-4 (Scheme 6b).[100] It is worth mentioning that the cross-coupling of aryl bromides with primary alcohols also proved viable under the electrochemical nickel catalysis.[99]

Based on detailed experimental and computational mechanistic investigations, a plausible catalytic cycle was proposed for the nickel-catalyzed electrochemical amination of aryl halides **12** (Scheme 7).[99] It was thus suggested to initiate by cathodic reduction of a dynamically ligated nickel(II) pre-catalyst to generate nickel(I) species **17.** Then, the rapid oxidative addition of aryl halide **12** to **17** results in the formation of nickel(III) intermediate **18,** which undergoes a second cathodic reduction to form a stable nickel(II) species **19.** Coordination of the amine **13** to **19** followed by rate-limiting deprotonation provides intermediate **20.** The anodic oxidation of **20** to nickel(III) complex **21,** followed by rapid reductive elimination furnishes the desired product **14** and regenerates the catalytically active nickel(I) species **17.**

The versatility of the electrochemical nickel catalysis in cross-coupling was recently showacsed by Leonél and coworkers.[101] The authors devised mild electro-assisted nickel catalysis for the synthesis of (hetero)arylphosphonates **23** from (hetero)aryl

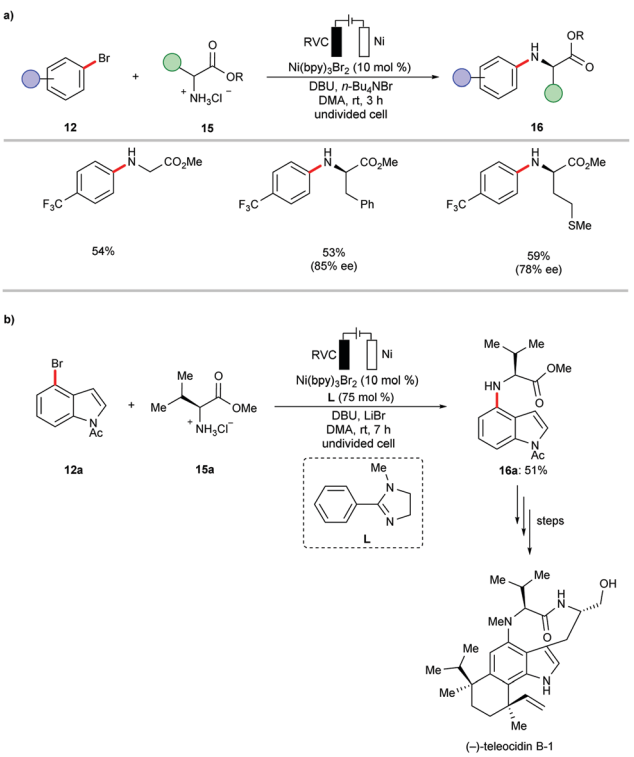

Scheme 6 Nickel-catalyzed electrochemical *N*-arylation of amino acid esters **15**.

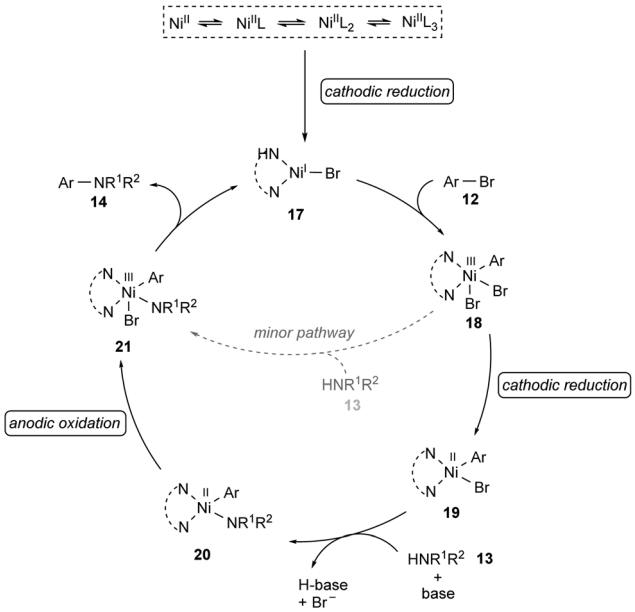

Scheme 7 Proposed mechanism for the electrochemical amination.

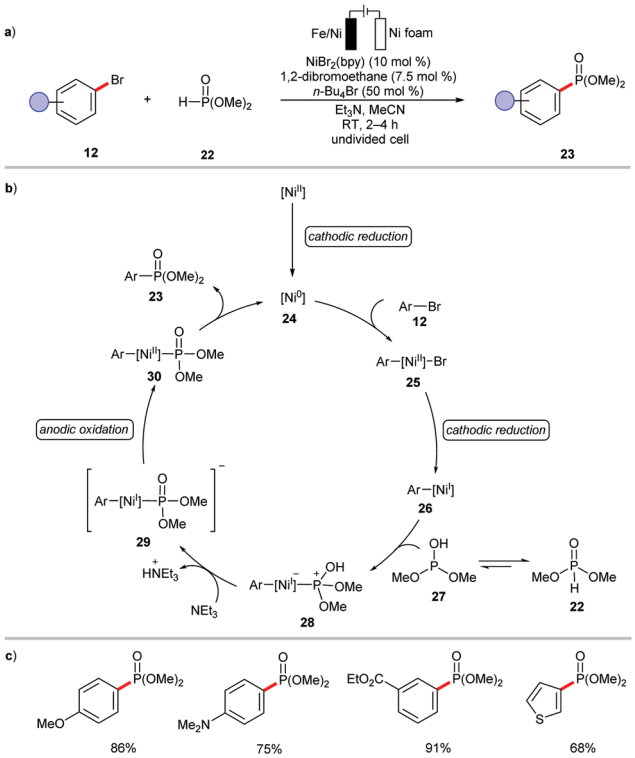

Scheme 8 Electrochemical nickel-catalyzed C–P couplings.

bromides **12** and dimethyl phosphite **22** (Scheme 8). However, the catalytic cycle was proposed to involve the *in situ* generation of catalytically active nickel(0) species **24.**

The reactivity of nickelaelectrocatalysis is not limited to C–N, C–O, and C–P bond formation. Indeed, the cross-coupling of thiols **32** with aryl iodides **31** was recently disclosed by Wang (Scheme 9).[102] The nickel-catalyzed C–S bond formation was

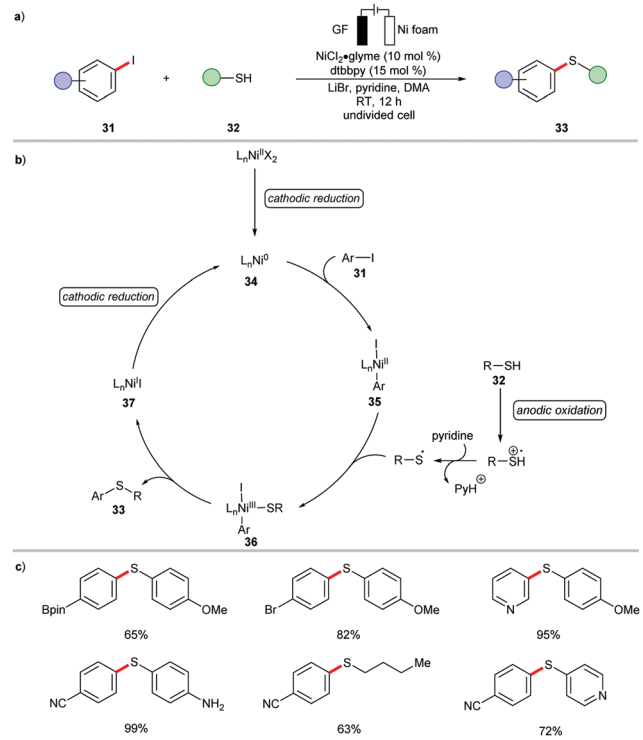

Scheme 9 Nickel-catalyzed electrochemical C–S formation.

realized at an ambient reaction temperature in presence of the air-stable nickel(II) pre-catalyst, $NiCl_2$·glyme. Both aryl- and alkyl thiols **32** were effectively converted under the reaction conditions to offer the desired thioethers **33** in excellent yields. Based on mechanistic findings, the catalytic mode of action was proposed to involve reductive elimination at the nickel(III) intermediate **36** (Scheme 9).[102]

4.3 Case study III: C–H activation

The merger of C–H activation and electrochemistry set the stage to establish new reactivities with high levels of resource economy. Despite indisputable advances, electrocatalytic organometallic C–H activations were thus far limited to precious palladium catalysts[103] and N-coordination as evidenced by Jutand,[103] Kakiuchi[104–107] and Mei,[108–111] among others.[52,109,112–115] Very recently, electrochemical organometallic C–H activation reactions employing rhodium(III),[116–120] iridium(III),[121,122] and less expensive ruthenium(II)[123–127] complexes have been accomplished by Ackermann and others. Hence, cost-intensive precious transition metals have until very recently proven mandatory. In contrast, we illustrate the huge potential of merging 3d metal catalysts with electrochemistry to achieve unprecedented reactivities in C–H activation reactions towards full resource economy.[56,128]

4.3.1 Cobaltaelectro-catalyzed C–H activation. In 2017, the Ackermann group reported the merger of cobalt-catalyzed C–H activation and electro-reoxidation of the cobalt catalyst as the key step of the catalytic cycle.[54] This proof of concept study realized the direct C–H oxygenation of aryl and alkenyl amides **38** with inexpensive and Earth-abundant $Co(OAc)_2{\cdot}4H_2O$ as the catalyst (Scheme 10). The key features of the method concerning resource economy include, (i) Earth-abundant 3d

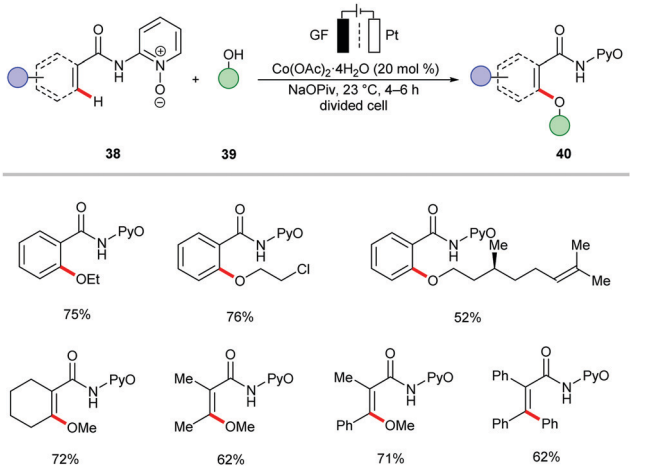

Scheme 10 C–H oxygenation *via* electrochemical cobalt catalysis.

metal catalyst, (ii) cost-effective commercial cobalt salt being devoid of the costly Cp*-ancillary ligand,[129,130] (iii) no stoichiometric, hazardous metal oxidants, (iv) ambient reaction temperature of 23 °C, and (v) benign H_2 as the sole by-product. Notably, the cobaltaelectro-catalyzed C–H oxygenation was also feasible in bio-based γ-valerolactone (GVL) as the solvent,[131,132] which further substantiated the green nature of the C–H activation protocol.[133] Based on detailed experimental studies and fully characterized cyclometalated intermediates of cobaltaelectro-catalyzed C–H activation, Ackermann proposed a plausible reaction pathway to involve a Co(III)/Co(IV)/Co(II) manifold.[134] (Scheme 11). The *N*,*O*-bidentate chelation-assisted *ortho*-C–H

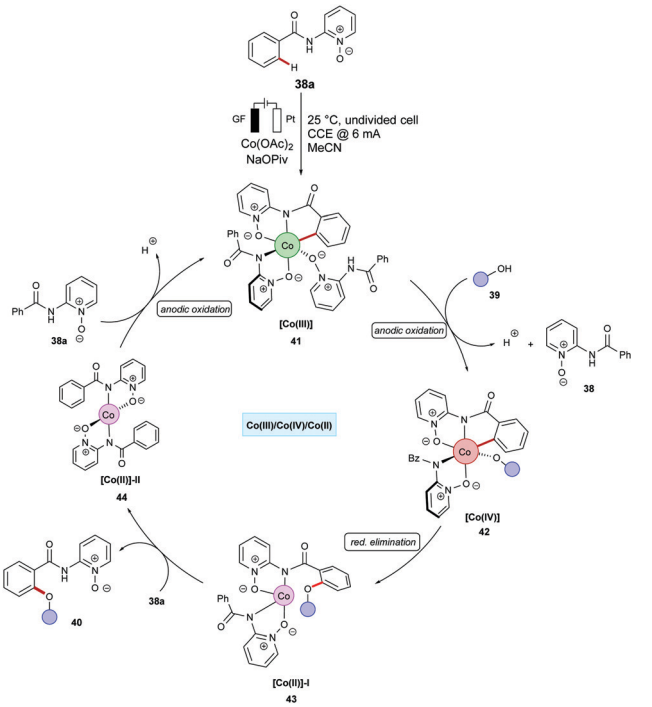

Scheme 11 Proposed catalytic cycle for the cobaltaelectro-catalyzed C–H oxygenation.

activation to form cobalt(III) intermediate **41** followed oxidation induced C–O bond forming reductive elimination from cobalt(IV) species **42** resulted the desired product **40** and the cobalt(II) complex **43**. The cobalt(II) species **44** is reoxidized to the active cobalt(III) species **41** by anodic oxidation. The detailed cyclovoltammetric studies unraveled the formation of a cobalt(III) and cobalt(IV) species by anodic oxidations. Thus, the oxidation potential of 1.19 V_{SCE} was determined for the oxidation of cobalt(II) to cobalt(III) from the mixture of $Co(OAc)_2$, and NaOPiv in MeOH, whereas the oxidation potential of cobalt(III) complex **41** was found to be $E_{p,ox}$ = 0.95 V_{SCE}.[134] The oxidation potential of substrate **38a** was found to be significantly higher (1.51 V_{SCE}) than that of cobalt(II)/cobalt(III) or cobalt(III)/cobalt(IV) redox potentials.[54]

The cobaltaelectro-catalyzed C–H activation was not limited to C–O bond forming reactions. Thus, Ackermann established an intermolecular C–H amination protocol under mild reaction conditions (Scheme 12).[135] A variety of benzamides **38** bearing pyridine *N*-oxide (PyO) substituents were efficiently *ortho*-aminated with secondary amines **13** to afford the desired products **45** in good yields, while liberating H_2 as the sole by-product. The formation of H_2 was unambiguously confirmed by headspace gas chromatography (GC), and could be utilized for future hydrogen evolution reaction strategies (HER). A related C–H amination of amides also proved viable using 8-aminoquinoline (AQ) as the bidentate directing group, as was reported by Lei.[136] Here, the cobalt catalyst showed better efficacy in a divided cell using MeCN as reaction medium at 65 °C.

The versatile electrochemical cobalt catalysis was further-applied to the synthesis of biologically relevant isoquinolones **47** and pyridones **48** from aromatic and vinylic amides **38**, respectively (Scheme 13).[137] The reaction occurred at ambient temperature in a water-based solvent mixture and displayed ample substrate scope with high yields. The robust cobalt-electrocatalysis manifold for C–H/N–H activation was also achieved in biomass-derived glycerol as reaction medium.[138]

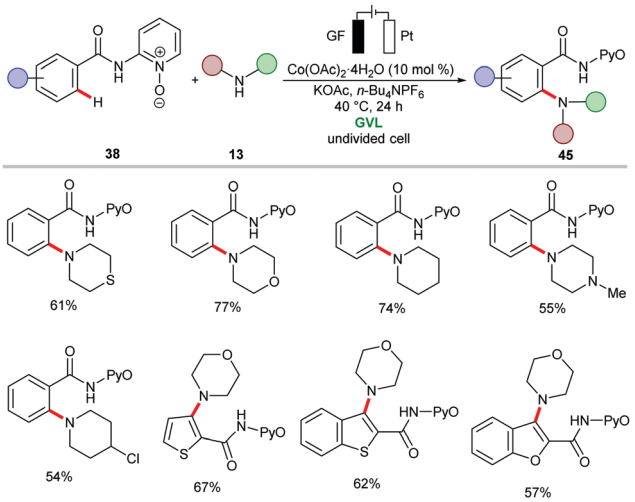

Scheme 12 Scope of cobaltaelectro-catalyzed C–H amination.

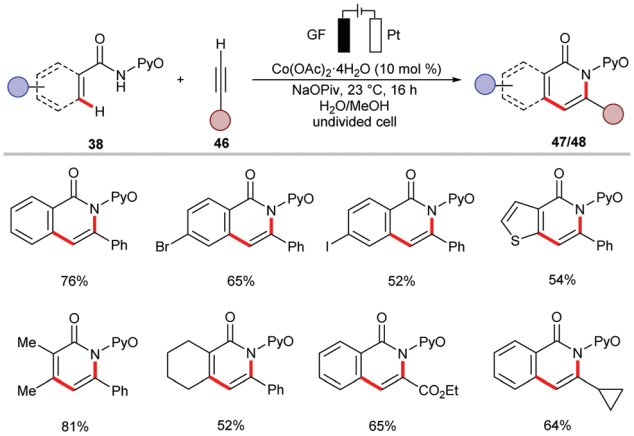

Scheme 13 Cobalt-catalyzed electrooxidative annulation reaction by amides **38** and alkenes **46**.

Remarkably, the resource economy of the transformation was substantiated by the direct use of renewable solar and wind energy.

Supported by competition experiments, KIE determination, and CV studies, a plausible reaction mechanism was proposed as shown in Scheme 14.[137] The anodically generated active cobalt(III) species **49** undergoes C–H cyclometallation to provide key intermediate **50**. Then, alkyne insertion into the C–Co bond followed by C–N bond forming reductive elimination delivers the desired product **47** and cobalt(I) species **52**. The electrochemical oxidation of **52** regenerates the active cobalt(III) species **49** and completes the catalytic cycle.

The cobalt-catalyzed electrochemical C–H/N–H annulation regime was until recently restricted to terminal alkynes **46**. In this context, the Ackermann group recently devised a protocol for the cobalt-catalyzed electrochemical C–H/N–H activation

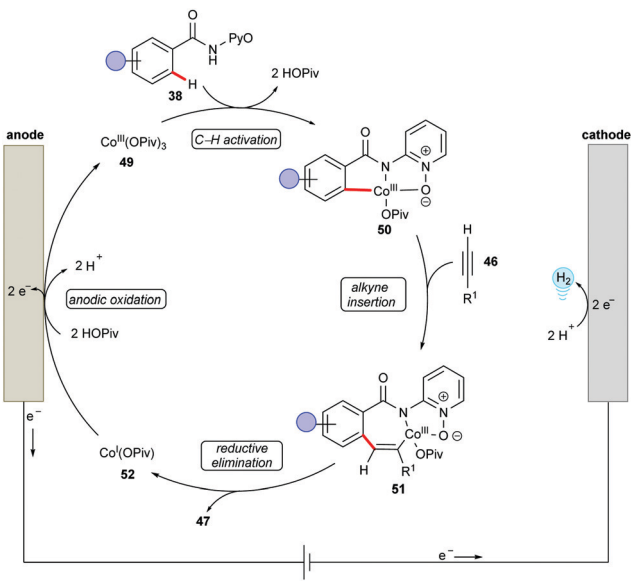

Scheme 14 Plausible catalytic cycle for the cobaltaelectro-catalyzed C–H/N–H annulation with terminal alkynes **46**.

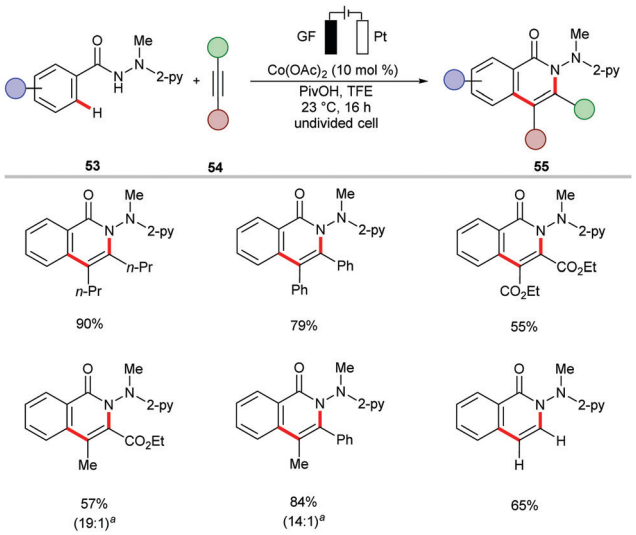

Scheme 15 Electrochemical C–H/N–H activation with internal alkynes **55**. [a] Ratio of regioisomers.

of pyridylbenzhydrazides **53** with internal alkynes **54** to access diversely substituted isoquinolones **55** (Scheme 15).[139] In the presence of catalytic amounts of $Co(OAc)_2$, a variety of internal alkynes **54** efficiently underwent [4+2] annulation with pyridylbenzhydrazides **53** at 23 °C. The unsymmetrically substituted internal alkynes **54** offered the desired products **55** with high levels of regioselectivity. Further, for the first time, the electrocatalytic removal of the directing group was realized through samarium-catalyzed cathodic reduction (Scheme 16).[139]

Next, the potency of cobaltaelectro-catalyzed C–H/N–H annulation was probed to include allenes[140–149] (Scheme 17).[150] The reaction was performed in a user-friendly undivided cell setup at 40 °C. The versatile cobalt catalysis transformed diversely substituted allenes **57** into the desired isoquinolones **58** in high yields. Notably, more challenging internal allenes **57** also proved viable substrates to deliver the corresponding *exo*-methylene isoquinolones **58**. Based on the detailed experimental and computational mechanistic investigations, a plausible catalytic was proposed as shown in Scheme 18. Anodically generated active cobalt(III) species **59** undergoes chelation assisted C–H cobaltation to give intermediate **60**. Allene precoordination followed by regioselective migratory insertion results in the

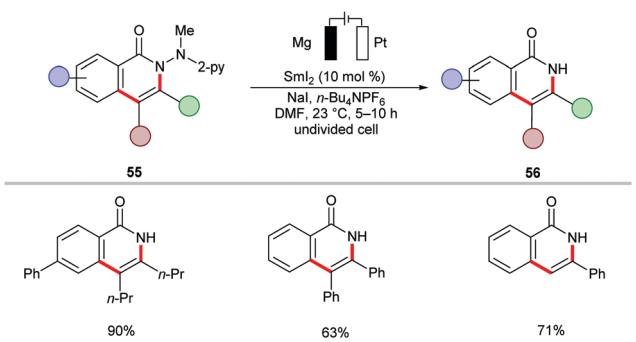

Scheme 16 Electroreductive removal of the directing group.

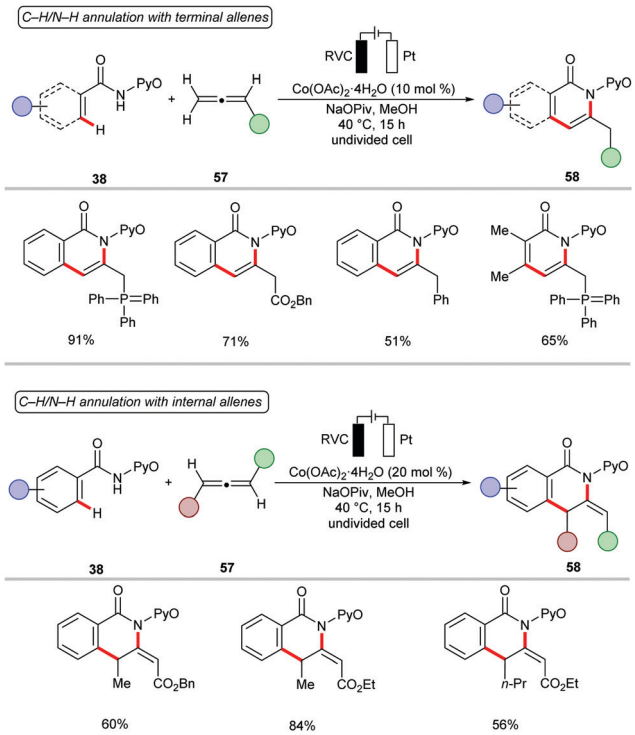

Scheme 17 Cobaltaelectro-catalyzed C–H/N–H activation of benz- and acrylamides **38** with allenes **57**.

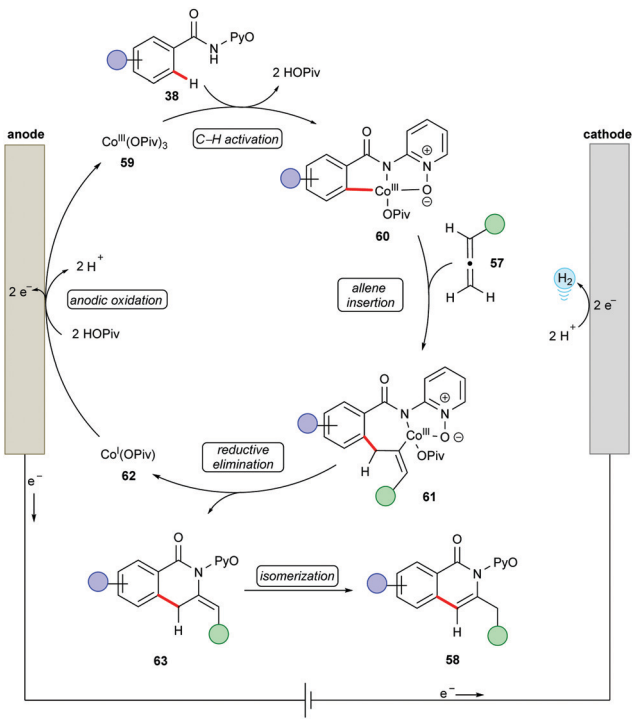

Scheme 18 Catalytic cycle for C–H/N–H activation with allenes **XX**.

seven-membered intermediate **61**. The *exo*-methylene isoquinolones **63** are generated upon reductive elimination. The catalytically active cobalt(III) species **59** is regenerated by anodic oxidation of cobalt(I) species **62**.

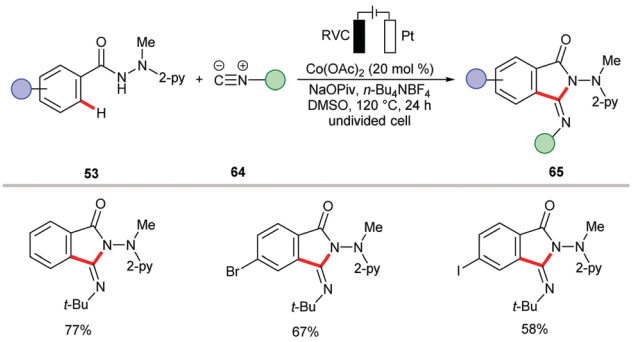

Scheme 19 Cobaltaelectro-catalyzed C–H/N–H annulation with isocyanides **64**.

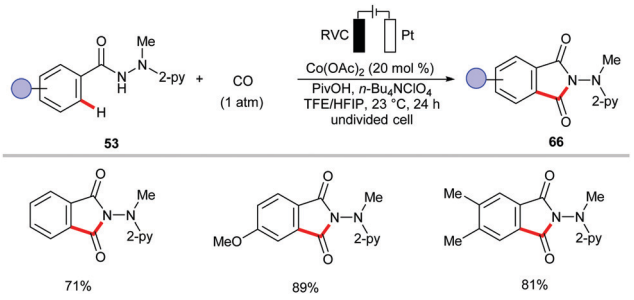

Scheme 20 Electrochemical C–H/N–H carbonylation at 23 °C.

The electrochemical cobalt-catalyzed C–H/N–H activation was further extended to a [4+1] annulation of benzhydrazides **53** with isocyanides **64** (Scheme 19).[151] Besides, the authors demonstrated the synthesis of phthalimide derivatives **66** *via* annulation of CO (1 atm) by benzhydrazides **53** at 23 °C in a user-friendly undivided cell (Scheme 20).[151] This approach was also realized by the group of Lei, albeit with 8-aminoquinoline as the directing group.[152]

4.3.2 Copper-catalyzed electrochemical C–H activation. Recently, Mei and coworkers successfully highlighted the efficacy of copper catalysis[153,154] in electrochemical C–H functionalizations (Scheme 21).[155] Here, catalytic amounts of $Cu(OTf)_2$ enabled the *ortho*-selective C–H amination of aryl amines **67** bearing the picolinamide (PA) directing group. The presence of *n*-Bu_4NI as the redox mediator was identified to be crucial for the amination protocol. Notably, the reaction could be performed in an undivided cell at 27 °C, without any electrodeposition of copper *via* cathodic reduction. A wide range of *n*-arylpicolinamides **67** was transformed into *ortho*-di-aminoarenes **68**. The detailed experimental studies suggested a single electron transfer (SET) mechanism to be operative in this reaction (Scheme 21).

In a subsequent report, Nicholls demonstrated a copper-catalyzed electrochemical C–H amination of benzamides **75** bearing a 8-AQ directing group.[156] The synthetic utility of the reaction was well explored for a series of amines containing active pharmaceutical ingredients (APIs) (Scheme 22).

The cupraelectro catalysis was not limited to C–H aminations. Indeed, the Ackermann group disclosed a first example

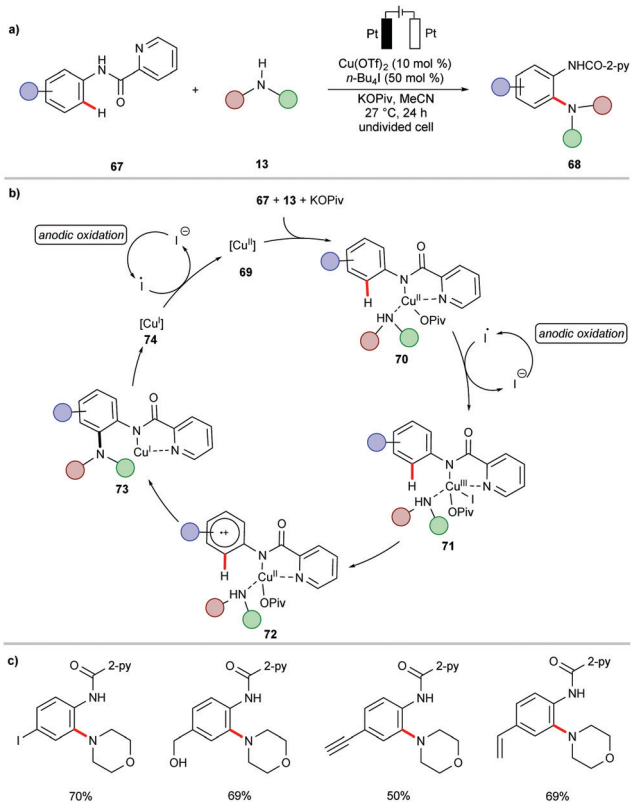

Scheme 21 Electrochemical copper-catalyzed C–H amination.

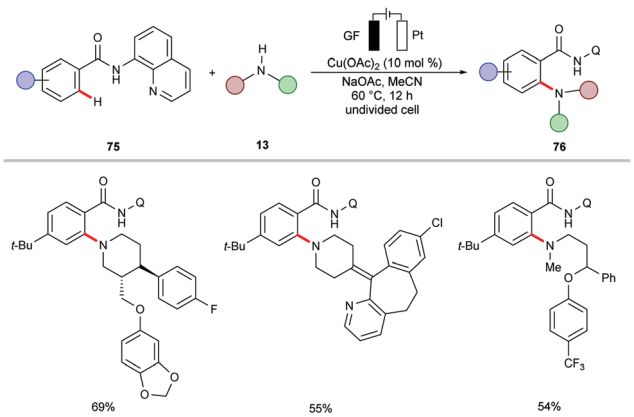

Scheme 22 Cupraelectro-catalyzed C–H amination with API molecules.

of cupraelectro-catalyzed alkyne annulation reaction with electricity as the terminal oxidant.[157] The transformation provided access to biologically relevant isoindolones **78** from benzamides **75** and terminal alkynes **46** *via* C–H/N–H functionalizations (Scheme 23). The robust cupraelectro-catalysis also proved applicable to alkynyl carboxylic acids **77** to give the desired products **78** in good yields through decarboxylative C–H/C–C cleavage.

Remarkably, the cupraelectro annulation contrasts with related cobaltaelectro annulations (*vide infra*, Schemes 13 and 15) for isoquinolones **47**/**55**,[137,139] delivered the five-membered isoindolones **78**. The detailed mechanistic studies including

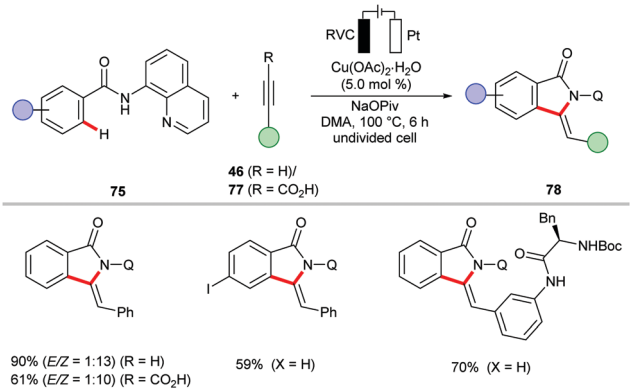

Scheme 23 Cupraelectro-catalyzed alkyne **46**/**77** annulation for isoindolone **78** formation.

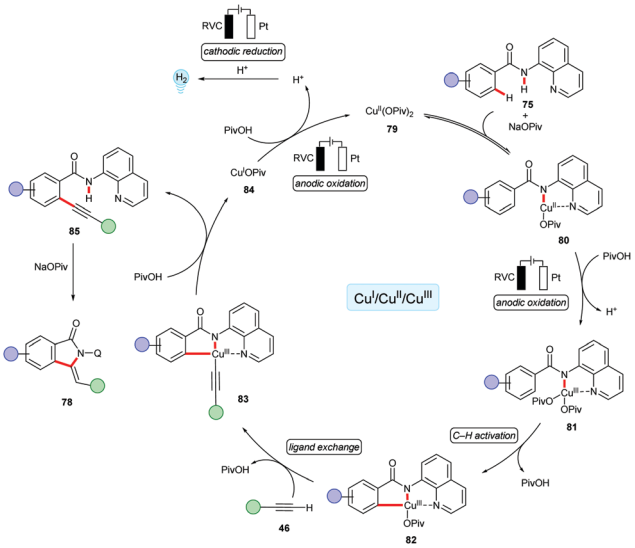

Scheme 24 Proposed catalytic cycle for the cupraelectro-catalyzed alkyne **46** annulation.

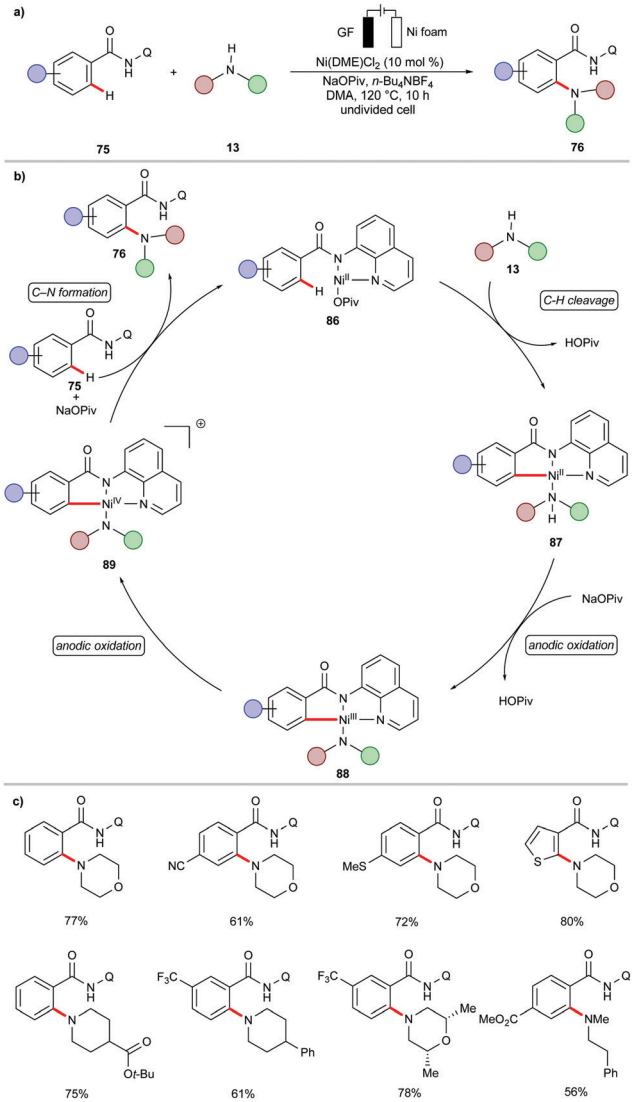

Scheme 25 Nickellaelectrocatalytic C–H amination.

competition experiments, KIE by *in operando* React-IR supported the C–H alkynylation mechanism *via* facile C–H scission (Scheme 24). The CV studies revealed an oxidation potential of 0.95 V_{SCE} for the oxidation of copper(II) to copper(III) from the mixture of the copper(II) catalyst and substrate **67** in DMA. The reoxidation of the copper(I) species to copper(II) readily occurred at 0.05 V_{SCE} as observed in CV data.[157] The formation of molecular hydrogen as the sole byproduct was confirmed.

4.3.3 Nickellaelectro-catalyzed C–H activation. In consideration of its Earth-abundance and economical reliability, nickel is often considered to be an alternative to expensive palladium catalysts. In this context, over the past few decades, a significant number of C–H activations have been realized employing nickel catalysis.[34] Despite this indisputable progress, electrochemical C–H activation with nickel catalysts remained elusive.

Very recently, the Ackermann group reported the first example of organometallic C–H activation for C–N formation by nickellaelectrocatalysis.[158] Thus, the *ortho*-selective C–H amination of amides **75** with a variety of secondary amines **13** was achieved using the commercially available nickel salt Ni(DME)Cl_2 (Scheme 25). The CV studies performed with a mixture of Ni(DME)Cl_2, NaOPiv and substrate **75** in DMA showed a redox potential of 0.26 V *vs.* Fc^+/Fc for the nickel(II)/nickel(III) event. Furthermore, the measurements after preheating at 120 °C for 30 min gave an oxidation wave at E_p = 0.49 V *vs.* $Fc^{+/0}$, which is indicative of a nickel(IV) species. Based on these CV data and other kinetic studies, the authors proposed a plausible reaction pathway to involve a Ni(III)/Ni(IV)/Ni(II) manifold (Scheme 25b).[158]

C–O forming transformations are of utmost importance for the synthesis of bioactive compounds, pharmaceuticals and functional materials.[159–162] In this context, the Ackermann group very recently devised a resource-economical nickellaelectrocatalysis strategy for the oxidative C–H alkoxylations with challenging secondary alcohols **91** with H_2 as the only stoichiometric byproduct *in lieu* of stoichiometric chemical oxidants (Scheme 26).[163] The reaction was conveniently achieved using inexpensive and bench-stable nickel salt Ni(DME)Cl_2 as the

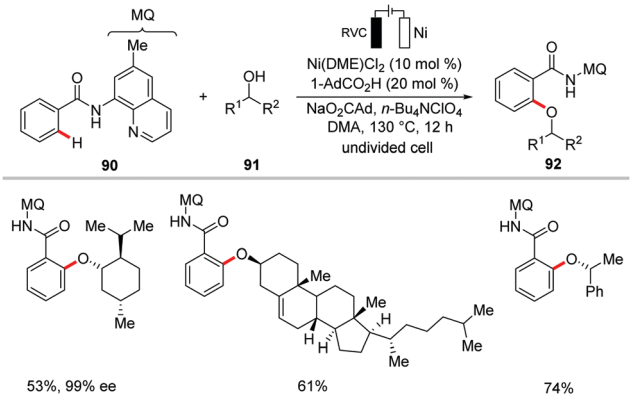

Scheme 26 Nickellaelectro-catalyzed secondary alkoxylation.

catalyst under economically robust undivided electrochemical cell setup. The versatile nickellaelectro-catalytic reaction conditions compatible with a wide variety of secondary alcohols including alicyclic, cyclic, benzylic and heterocyclic alcohols to give the desired alkoxylation products in excellent yields. Notably, the naturally-occurring alcohols menthol, cholesterol and β-estradiol were found to be compatible without racemization at the stereogenic centers.

4.3.4 Ferraelectro-catalyzed C–H activation. During the last decade, iron catalysts have been considered as an outstanding approach for sustainable molecular syntheses *via* C–H activation, because of its natural Earth-abundance, low toxicity and cost-effective nature.[34,164,165] Despite indisputable advances, the iron-catalyzed oxidative C–H transformation reactions strongly relied on superstoichiometric amounts of expensive 1,2-dichloroisobutane (DCIB) as the sacrificial oxidant. To overcome this major limitation, the Ackermann group disclosed the unprecedented ferraelectro catalytic approach for oxidative C–H activation.[166] Here, the regioselective ortho C–H arylation of amides **93** was achieved under DCIB-free reaction conditions using electricity as environmentally-benign oxidant (Scheme 27). Detailed experimental, spectroscopic, and DFT mechanistic studies yielded insights into an electrooxidative iron(II/III/I) manifold.

4.3.5 Manganaelectro-catalyzed C–H activation. The sustainable electrochemical organometallic C–H activation was furthermore put into practice in the presence of readily accessible, inexpensive manganese catalysts. As a proof of

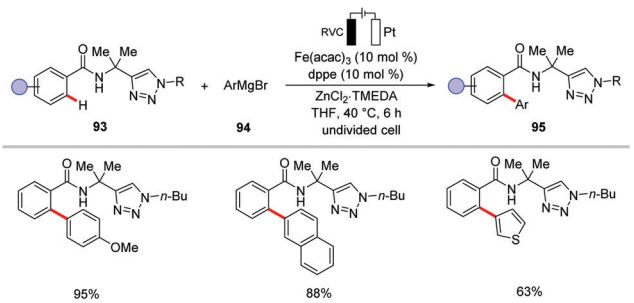

Scheme 27 Iron-catalyzed electrochemical C–H arylation.

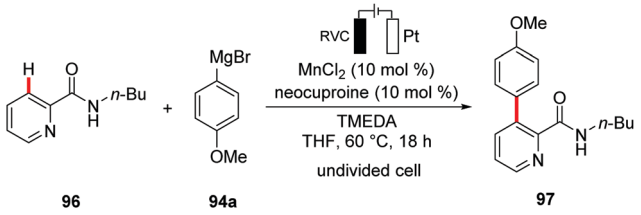

Scheme 28 Manganaelectro-catalyzed C–H arylation.

concept, Ackermann showcased the potential of the merger of manganese catalysis with electrocatalysis for the arylation of unactivated C(sp^2)–H bonds.[166] Thus, regioselective C3 arylation of picolinamides **96** was accomplished under mild manganaelectro-catalysis (Scheme 28).

5. Conclusions

Resource economy in molecular syntheses has gained significant momentum in recent years concerning the rising demand for sustainable strategies for molecular syntheses. The merger of electrochemistry with Earth-abundant 3d metal catalysis enabled the construction of challenging C–C and C–heteroatom bonds for complex organic molecules in a sustainable fashion under exceedingly mild reaction conditions. The metallaelectrocatalysis utilizes electro-oxidation/reduction in lieu of reactive chemical redox reagents, and thereby prevents undesired waste formation. Particularly, electricity from renewable energy sources, such as solar and wind power, features unique potential for the ideal step and redox economy. The potential of sustainable electrochemical 3d metal catalysis in molecular synthesis is herein highlighted with three key case studies. Thus, the recent developments of alkene difunctionalizations by manganese catalysts under electrochemical conditions set the stage for the syntheses of synthetically meaningful vicinally difunctionalized products (Case Study I). Electrochemical nickel-catalyzed cross-couplings proceeded under ambient reaction conditions to forge C–N, C–S and C–P bonds (Case Study II). Remarkably, the merger of 3d metal electrochemistry and C–H activation enabled excellent oxidant economy by using electricity as green oxidant and generates molecular hydrogen as the sole by-product (Case Study III). The metallaelectrocatalysis using 3d metal catalysts, such as cobalt, copper, nickel, iron and manganese, proceeded under mild reaction conditions with broad substrate scope. These metallaelectro-catalyzed C–H activations often proceeded in green reaction media, ensuring the high levels of sustainability. In sharp contrast to noble metal electrocatalyses,[103,107,110,111,167,168] most of the 3d metallaelectro-catalyzed organic syntheses could be accomplished in an user-friendly, undivided electrochemical cell setup. Likewise, the electrochemical cross-couplings by nickel catalyst involving cathodic reduction of the metal catalyst were conveniently performed in an undivided cell, provided that nickel electrodes were used (Case Study II). Given the unique features of 3d metallaelectrocatalysis in terms of resource economy, further advances are expected in this rapidly emerging research area,

including enantioselective transformations, dual metallaelectrocatalysis, and electrocatalytic C–C and C–heteroatom activations.

Conflicts of interest

There are no conflicts to declare.

Acknowledgements

Generous support by the Alexander von Humboldt Foundation (fellowship to P. G.), the DFG (Gottfried-Wilhelm-Leibniz-award to L. A. and SPP1807) is gratefully acknowledged.

Notes and references

1 S. A. Matlin, G. Mehta, H. Hopf and A. Krief, *Nat. Chem.*, 2016, **8**, 393–398.
2 B. Trost, *Science*, 1991, **254**, 1471–1477.
3 B. M. Trost, *Angew. Chem., Int. Ed. Engl.*, 1995, **34**, 259–281.
4 P. T. Anastas and J. C. Warner, *Green Chemistry: Theory and Practice*, Oxford University Press, Oxford, 1998.
5 P. A. Wender, M. P. Croatt and B. Witulski, *Tetrahedron*, 2006, **62**, 7505–7511.
6 N. Z. Burns, P. S. Baran and R. W. Hoffmann, *Angew. Chem., Int. Ed.*, 2009, **48**, 2854–2867.
7 T. Newhouse, P. S. Baran and R. W. Hoffmann, *Chem. Soc. Rev.*, 2009, **38**, 3010–3021.
8 T. H. Meyer, L. H. Finger, P. Gandeepan and L. Ackermann, *Trends Chem.*, 2019, **1**, 63–76.
9 W. Wang, M. M. Lorion, J. Shah, A. R. Kapdi and L. Ackermann, *Angew. Chem., Int. Ed.*, 2018, **57**, 14700–14717.
10 Z. Chen, M.-Y. Rong, J. Nie, X.-F. Zhu, B.-F. Shi and J.-A. Ma, *Chem. Soc. Rev.*, 2019, **48**, 4921–4942.
11 H. M. L. Davies and K. Liao, *Nat. Rev. Chem.*, 2019, **3**, 347–360.
12 C. He, W. G. Whitehurst and M. J. Gaunt, *Chem*, 2019, **5**, 1031–1058.
13 G. Liao, T. Zhou, Q.-J. Yao and B.-F. Shi, *Chem. Commun.*, 2019, **55**, 8514–8523.
14 S. Rej and N. Chatani, *Angew. Chem., Int. Ed.*, 2019, **58**, 8304–8329.
15 S. Santoro, F. Ferlin, L. Ackermann and L. Vaccaro, *Chem. Soc. Rev.*, 2019, **48**, 2767–2782.
16 R. Szpera, D. F. J. Moseley, L. B. Smith, A. J. Sterling and V. Gouverneur, *Angew. Chem., Int. Ed.*, 2019, **58**, 14824–14848.
17 H. Wang, X. Gao, Z. Lv, T. Abdelilah and A. Lei, *Chem. Rev.*, 2019, **119**, 6769–6787.
18 J. He, M. Wasa, K. S. L. Chan, Q. Shao and J.-Q. Yu, *Chem. Rev.*, 2017, **117**, 8754–8786.
19 M. Oelgemöller, *Chem. Rev.*, 2016, **116**, 9664–9682.
20 G. D. Scholes, G. R. Fleming, A. Olaya-Castro and R. van Grondelle, *Nat. Chem.*, 2011, **3**, 763–774.
21 D. M. Schultz and T. P. Yoon, *Science*, 2014, **343**, 1239176.
22 P. Gandeepan and L. Ackermann, *Chem*, 2018, **4**, 199–222.
23 Y. Yang, J. Lan and J. You, *Chem. Rev.*, 2017, **117**, 8787–8863.
24 Y. Wei, P. Hu, M. Zhang and W. Su, *Chem. Rev.*, 2017, **117**, 8864–8907.
25 Z. Dong, Z. Ren, S. J. Thompson, Y. Xu and G. Dong, *Chem. Rev.*, 2017, **117**, 9333–9403.
26 F. Wang, S. Yu and X. Li, *Chem. Soc. Rev.*, 2016, **45**, 6462–6477.
27 T. Gensch, M. N. Hopkinson, F. Glorius and J. Wencel-Delord, *Chem. Soc. Rev.*, 2016, **45**, 2900–2936.
28 H. M. L. Davies and D. Morton, *ACS Cent. Sci.*, 2017, **3**, 936–943.
29 P. Gandeepan and C.-H. Cheng, *Chem. – Asian J.*, 2015, **10**, 824–838.
30 T. W. Lyons and M. S. Sanford, *Chem. Rev.*, 2010, **110**, 1147–1169.
31 D. A. Colby, R. G. Bergman and J. A. Ellman, *Chem. Rev.*, 2010, **110**, 624–655.
32 R. Giri, B.-F. Shi, K. M. Engle, N. Maugel and J.-Q. Yu, *Chem. Soc. Rev.*, 2009, **38**, 3242–3272.
33 L. Ackermann, R. Vicente and A. R. Kapdi, *Angew. Chem., Int. Ed.*, 2009, **48**, 9792–9826.
34 P. Gandeepan, T. Müller, D. Zell, G. Cera, S. Warratz and L. Ackermann, *Chem. Rev.*, 2019, **119**, 2192–2452.
35 P. Gandeepan and L. Ackermann, in *Non-Noble Metal Catalysis: Molecular Approaches and Reactions*, ed. R. J. K. Gebbink and M.-E. Moret, Wiley-VCH, Weinheim, 2019, pp. 391–423.
36 Z. Shi, C. Zhang, C. Tang and N. Jiao, *Chem. Soc. Rev.*, 2012, **41**, 3381–3430.
37 S. S. Stahl, *Angew. Chem., Int. Ed.*, 2004, **43**, 3400–3420.
38 A. Bechtoldt, C. Tirler, K. Raghuvanshi, S. Warratz, C. Kornhaaß and L. Ackermann, *Angew. Chem., Int. Ed.*, 2016, **55**, 264–267.
39 P. M. Osterberg, J. K. Niemeier, C. J. Welch, J. M. Hawkins, J. R. Martinelli, T. E. Johnson, T. W. Root and S. S. Stahl, *Org. Process Res. Dev.*, 2015, **19**, 1537–1543.
40 J. Twilton, C. Le, P. Zhang, M. H. Shaw, R. W. Evans and D. W. C. MacMillan, *Nat. Rev. Chem.*, 2017, **1**, 0052.
41 R. C. McAtee, E. J. McClain and C. R. J. Stephenson, *Trends Chem.*, 2019, **1**, 111–125.
42 N. A. Romero and D. A. Nicewicz, *Chem. Rev.*, 2016, **116**, 10075–10166.
43 D. C. Miller, K. T. Tarantino and R. R. Knowles, *Top. Curr. Chem.*, 2016, **374**, 30.
44 K. L. Skubi, T. R. Blum and T. P. Yoon, *Chem. Rev.*, 2016, **116**, 10035–10074.
45 L. Marzo, S. K. Pagire, O. Reiser and B. König, *Angew. Chem., Int. Ed.*, 2018, **57**, 10034–10072.
46 D. C. Fabry and M. Rueping, *Acc. Chem. Res.*, 2016, **49**, 1969–1979.
47 M. Yan, Y. Kawamata and P. S. Baran, *Chem. Rev.*, 2017, **117**, 13230–13319.
48 S. Möhle, M. Zirbes, E. Rodrigo, T. Gieshoff, A. Wiebe and S. R. Waldvogel, *Angew. Chem., Int. Ed.*, 2018, **57**, 6018–6041.
49 J.-i. Yoshida, K. Kataoka, R. Horcajada and A. Nagaki, *Chem. Rev.*, 2008, **108**, 2265–2299.

50 A. Jutand, *Chem. Rev.*, 2008, **108**, 2300–2347.
51 N. Sauermann, T. H. Meyer, Y. Qiu and L. Ackermann, *ACS Catal.*, 2018, **8**, 7086–7103.
52 C. Ma, P. Fang and T.-S. Mei, *ACS Catal.*, 2018, **8**, 7179–7189.
53 S. Tang, Y. Liu and A. Lei, *Chem*, 2018, **4**, 27–45.
54 N. Sauermann, T. H. Meyer, C. Tian and L. Ackermann, *J. Am. Chem. Soc.*, 2017, **139**, 18452–18455.
55 K. S. Egorova and V. P. Ananikov, *Organometallics*, 2017, **36**, 4071–4090.
56 N. Sauermann, T. H. Meyer and L. Ackermann, *Chem. – Eur. J.*, 2018, **24**, 16209–16217.
57 A. Volta, *Philos. Trans. R. Soc. London*, 1800, **90**, 403–431.
58 M. Faraday, *Ann. Phys.*, 1834, **109**, 433–451.
59 H. Kolbe, *Justus Liebigs Ann. Chem.*, 1849, **69**, 257–294.
60 O. R. Luca, J. L. Gustafson, S. M. Maddox, A. Q. Fenwick and D. C. Smith, *Org. Chem. Front.*, 2015, **2**, 823–848.
61 In the following text, for the sake of simplicity only the oxidation half-reaction will be used as an example. All general principles are equally valid for the cathodic reduction half-reaction.
62 R. Francke and R. D. Little, *Chem. Soc. Rev.*, 2014, **43**, 2492–2521.
63 G. S. Sauer and S. Lin, *ACS Catal.*, 2018, **8**, 5175–5187.
64 L. Wang, C. Qi, T. Guo and H. Jiang, *Org. Lett.*, 2019, **21**, 2223–2226.
65 Y.-X. Dong, Y. Li, C.-C. Gu, S.-S. Jiang, R.-J. Song and J.-H. Li, *Org. Lett.*, 2018, **20**, 7594–7597.
66 A. Bunescu, T. M. Ha, Q. Wang and J. Zhu, *Angew. Chem., Int. Ed.*, 2017, **56**, 10555–10558.
67 J. Waser, H. Nambu and E. M. Carreira, *J. Am. Chem. Soc.*, 2005, **127**, 8294–8295.
68 X. Sun, X. Li, S. Song, Y. Zhu, Y.-F. Liang and N. Jiao, *J. Am. Chem. Soc.*, 2015, **137**, 6059–6066.
69 R. Zhu and S. L. Buchwald, *J. Am. Chem. Soc.*, 2015, **137**, 8069–8077.
70 K. Shen and Q. Wang, *J. Am. Chem. Soc.*, 2017, **139**, 13110–13116.
71 B. B. Snider and J. R. Duvall, *Org. Lett.*, 2004, **6**, 1265–1268.
72 B. Zhang and A. Studer, *Org. Lett.*, 2014, **16**, 1790–1793.
73 Y.-A. Yuan, D.-F. Lu, Y.-R. Chen and H. Xu, *Angew. Chem., Int. Ed.*, 2016, **55**, 534–538.
74 B. H. Nguyen, A. Redden and K. D. Moeller, *Green Chem.*, 2014, **16**, 69–72.
75 H. Tanaka, M. Kuroboshi, H. Takeda, H. Kanda and S. Torii, *J. Electroanal. Chem.*, 2001, **507**, 75–81.
76 S. Torii, P. Liu, N. Bhuvaneswari, C. Amatore and A. Jutand, *J. Org. Chem.*, 1996, **61**, 3055–3060.
77 S. Torii, P. Liu and H. Tanaka, *Chem. Lett.*, 1995, 319–320.
78 N. Fu, G. S. Sauer, A. Saha, A. Loo and S. Lin, *Science*, 2017, **357**, 575–579.
79 N. Fu, G. S. Sauer and S. Lin, *J. Am. Chem. Soc.*, 2017, **139**, 15548–15553.
80 J. C. Siu, J. B. Parry and S. Lin, *J. Am. Chem. Soc.*, 2019, **141**, 2825–2831.
81 K.-Y. Ye, G. Pombar, N. Fu, G. S. Sauer, I. Keresztes and S. Lin, *J. Am. Chem. Soc.*, 2018, **140**, 2438–2441.
82 K.-Y. Ye, Z. Song, G. S. Sauer, J. H. Harenberg, N. Fu and S. Lin, *Chem. – Eur. J.*, 2018, **24**, 12274–12279.
83 N. Fu, Y. Shen, A. R. Allen, L. Song, A. Ozaki and S. Lin, *ACS Catal.*, 2018, **9**, 746–754.
84 F. Diederich and P. J. Stang, *Metal-Catalyzed Cross-Coupling Reactions*, Wiley-VCH, New York, 1998.
85 A. Suzuki, *Angew. Chem., Int. Ed.*, 2011, **50**, 6722–6737.
86 E. Negishi, *Angew. Chem., Int. Ed.*, 2011, **50**, 6738–6764.
87 C. C. C. Johansson Seechurn, M. O. Kitching, T. J. Colacot and V. Snieckus, *Angew. Chem., Int. Ed.*, 2012, **51**, 5062–5085.
88 D. G. Brown and J. Boström, *J. Med. Chem.*, 2015, **59**, 4443–4458.
89 P. Ruiz-Castillo and S. L. Buchwald, *Chem. Rev.*, 2016, **116**, 12564–12649.
90 J. F. Hartwig, *Angew. Chem., Int. Ed.*, 1998, **37**, 2046–2067.
91 E. C. Hughes, F. Veatch and V. Elersich, *Ind. Eng. Chem.*, 1950, **42**, 787–790.
92 R. Cramer and D. R. Coulson, *J. Org. Chem.*, 1975, **40**, 2267–2273.
93 J. P. Wolfe and S. L. Buchwald, *J. Am. Chem. Soc.*, 1997, **119**, 6054–6058.
94 S. Ge, R. A. Green and J. F. Hartwig, *J. Am. Chem. Soc.*, 2014, **136**, 1617–1627.
95 N. F. Fine Nathel, J. Kim, L. Hie, X. Jiang and N. K. Garg, *ACS Catal.*, 2014, **4**, 3289–3293.
96 M. Marín, R. J. Rama and M. C. Nicasio, *Chem. Rec.*, 2016, **16**, 1819–1832.
97 C. Gosmini, J. Y. Nédélec and J. Périchon, *Tetrahedron Lett.*, 2000, **41**, 201–203.
98 C. Li, Y. Kawamata, H. Nakamura, J. C. Vantourout, Z. Liu, Q. Hou, D. Bao, J. T. Starr, J. Chen, M. Yan and P. S. Baran, *Angew. Chem., Int. Ed.*, 2017, **56**, 13088–13093.
99 Y. Kawamata, J. C. Vantourout, D. P. Hickey, P. Bai, L. Chen, Q. Hou, W. Qiao, K. Barman, M. A. Edwards, A. F. Garrido-Castro, J. N. deGruyter, H. Nakamura, K. Knouse, C. Qin, K. J. Clay, D. Bao, C. Li, J. T. Starr, C. Garcia-Irizarry, N. Sach, H. S. White, M. Neurock, S. D. Minteer and P. S. Baran, *J. Am. Chem. Soc.*, 2019, **141**, 6392–6402.
100 H. Nakamura, K. Yasui, Y. Kanda and P. S. Baran, *J. Am. Chem. Soc.*, 2019, **141**, 1494–1497.
101 S. Sengmany, A. Ollivier, E. Le Gall and E. Léonel, *Org. Biomol. Chem.*, 2018, **16**, 4495–4500.
102 Y. Wang, L. Deng, X. Wang, Z. Wu, Y. Wang and Y. Pan, *ACS Catal.*, 2019, **9**, 1630–1634.
103 C. Amatore, C. Cammoun and A. Jutand, *Adv. Synth. Catal.*, 2007, **349**, 292–296.
104 M. Konishi, K. Tsuchida, K. Sano, T. Kochi and F. Kakiuchi, *J. Org. Chem.*, 2017, **82**, 8716–8724.
105 F. Saito, H. Aiso, T. Kochi and F. Kakiuchi, *Organometallics*, 2014, **33**, 6704–6707.
106 H. Aiso, T. Kochi, H. Mutsutani, T. Tanabe, S. Nishiyama and F. Kakiuchi, *J. Org. Chem.*, 2012, **77**, 7718–7724.
107 F. Kakiuchi, T. Kochi, H. Mutsutani, N. Kobayashi, S. Urano, M. Sato, S. Nishiyama and T. Tanabe, *J. Am. Chem. Soc.*, 2009, **131**, 11310–11311.

108 C. Ma, C.-Q. Zhao, Y.-Q. Li, L.-P. Zhang, X.-T. Xu, K. Zhang and T.-S. Mei, *Chem. Commun.*, 2017, **53**, 12189–12192.
109 K.-J. Jiao, C.-Q. Zhao, P. Fang and T.-S. Mei, *Tetrahedron Lett.*, 2017, **58**, 797–802.
110 Y.-Q. Li, Q.-L. Yang, P. Fang, T.-S. Mei and D. Zhang, *Org. Lett.*, 2017, **19**, 2905–2908.
111 Q.-L. Yang, Y.-Q. Li, C. Ma, P. Fang, X.-J. Zhang and T.-S. Mei, *J. Am. Chem. Soc.*, 2017, **139**, 3293–3298.
112 F. Kakiuchi and T. Kochi, *Isr. J. Chem.*, 2017, **57**, 953–963.
113 Y. Budnikova, Y. Dudkina and M. Khrizanforov, *Inorganics*, 2017, **5**, 70.
114 J. Chen, S. Lv and S. Tian, *ChemSusChem*, 2018, **12**, 115–132.
115 N. Sauermann, T. H. Meyer, Y. Qiu and L. Ackermann, *ACS Catal.*, 2018, **8**, 7086–7103.
116 Y. Qiu, W.-J. Kong, J. Struwe, N. Sauermann, T. Rogge, A. Scheremetjew and L. Ackermann, *Angew. Chem., Int. Ed.*, 2018, **57**, 5828–5832.
117 W. J. Kong, L. H. Finger, J. C. A. Oliveira and L. Ackermann, *Angew. Chem., Int. Ed.*, 2019, **58**, 6342–6346.
118 Y. Qiu, A. Scheremetjew and L. Ackermann, *J. Am. Chem. Soc.*, 2019, **141**, 2731–2738.
119 W.-J. Kong, L. H. Finger, A. M. Messinis, R. Kuniyil, J. C. A. Oliveira and L. Ackermann, *J. Am. Chem. Soc.*, 2019, **141**, 17198–17206.
120 W.-J. Kong, Z. Shen, L. H. Finger and L. Ackermann, *Angew. Chem., Int. Ed.*, 2020, **59**, 5551–5556.
121 Y. Qiu, M. Stangier, T. H. Meyer, J. C. A. Oliveira and L. Ackermann, *Angew. Chem., Int. Ed.*, 2018, **57**, 14179–14183.
122 Q.-L. Yang, Y.-K. Xing, X.-Y. Wang, H.-X. Ma, X.-J. Weng, X. Yang, H.-M. Guo and T.-S. Mei, *J. Am. Chem. Soc.*, 2019, **141**, 18970–18976.
123 Y. Qiu, C. Tian, L. Massignan, T. Rogge and L. Ackermann, *Angew. Chem., Int. Ed.*, 2018, **57**, 5818–5822.
124 R. Mei, J. Koeller and L. Ackermann, *Chem. Commun.*, 2018, **54**, 12879–12882.
125 F. Xu, Y.-J. Li, C. Huang and H.-C. Xu, *ACS Catal.*, 2018, **8**, 3820–3824.
126 M.-J. Luo, M. Hu, R.-J. Song, D.-L. He and J.-H. Li, *Chem. Commun.*, 2019, **55**, 1124–1127.
127 L. Massignan, X. Tan, T. H. Meyer, R. Kuniyil, A. M. Messinis and L. Ackermann, *Angew. Chem., Int. Ed.*, 2020, **59**, 3184–3189.
128 L. Ackermann, *Acc. Chem. Res.*, 2020, **53**, 84–104.
129 M. Moselage, J. Li and L. Ackermann, *ACS Catal.*, 2016, **6**, 498–525.
130 T. Andou, Y. Saga, H. Komai, S. Matsunaga and M. Kanai, *Angew. Chem., Int. Ed.*, 2013, **52**, 3213–3216.
131 S. Santoro, A. Marrocchi, D. Lanari, L. Ackermann and L. Vaccaro, *Chem. – Eur. J.*, 2018, **24**, 13383–13390.
132 P. Gandeepan, N. Kaplaneris, S. Santoro, L. Vaccaro and L. Ackermann, *ACS Sustainable Chem. Eng.*, 2019, **7**, 8023–8040.
133 C. Tian, U. Dhawa, J. Struwe and L. Ackermann, *Chin. J. Chem.*, 2019, **37**, 552–556.
134 T. H. Meyer, J. C. A. de Oliveira, D. Ghorai and L. Ackermann, *Angew. Chem., Int. Ed.*, 2020, DOI: 10.1002/ange.202002258.
135 N. Sauermann, R. Mei and L. Ackermann, *Angew. Chem., Int. Ed.*, 2018, **57**, 5090–5094.
136 X. Gao, P. Wang, L. Zeng, S. Tang and A. Lei, *J. Am. Chem. Soc.*, 2018, **140**, 4195–4199.
137 C. Tian, L. Massignan, T. H. Meyer and L. Ackermann, *Angew. Chem., Int. Ed.*, 2018, **57**, 2383–2387.
138 T. H. Meyer, G. A. Chesnokov and L. Ackermann, *ChemSusChem*, 2020, **13**, 668–671.
139 R. Mei, N. Sauermann, J. C. A. Oliveira and L. Ackermann, *J. Am. Chem. Soc.*, 2018, **140**, 7913–7921.
140 J. Mo, T. Müller, J. C. A. Oliveira and L. Ackermann, *Angew. Chem., Int. Ed.*, 2018, **57**, 7719–7723.
141 S. Nakanowatari, T. Müller, J. C. A. Oliveira and L. Ackermann, *Angew. Chem., Int. Ed.*, 2017, **56**, 15891–15895.
142 S. Nakanowatari, R. Mei, M. Feldt and L. Ackermann, *ACS Catal.*, 2017, **7**, 2511–2515.
143 R. Boobalan, R. Kuppusamy, R. Santhoshkumar, P. Gandeepan and C.-H. Cheng, *ChemCatChem*, 2017, **9**, 273–277.
144 N. Thrimurtulu, A. Dey, D. Maiti and C. M. R. Volla, *Angew. Chem., Int. Ed.*, 2016, **55**, 12361–12365.
145 P. Gandeepan, P. Rajamalli and C.-H. Cheng, *Chem. – Eur. J.*, 2015, **21**, 9198–9203.
146 R. Zeng, J. Ye, C. Fu and S. Ma, *Adv. Synth. Catal.*, 2013, **355**, 1963–1970.
147 B. Ye and N. Cramer, *J. Am. Chem. Soc.*, 2013, **135**, 636–639.
148 R. Zeng, C. Fu and S. Ma, *J. Am. Chem. Soc.*, 2012, **134**, 9597–9600.
149 Y. J. Zhang, E. Skucas and M. J. Krische, *Org. Lett.*, 2009, **11**, 4248–4250.
150 T. H. Meyer, J. C. A. Oliveira, S. C. Sau, N. W. J. Ang and L. Ackermann, *ACS Catal.*, 2018, **8**, 9140–9147.
151 S. C. Sau, R. Mei, J. Struwe and L. Ackermann, *ChemSusChem*, 2019, **12**, 3023–3027.
152 L. Zeng, H. Li, S. Tang, X. Gao, Y. Deng, G. Zhang, C.-W. Pao, J.-L. Chen, J.-F. Lee and A. Lei, *ACS Catal.*, 2018, **8**, 5448–5453.
153 O. Daugulis, H.-Q. Do and D. Shabashov, *Acc. Chem. Res.*, 2009, **42**, 1074–1086.
154 A. E. Wendlandt, A. M. Suess and S. S. Stahl, *Angew. Chem., Int. Ed.*, 2011, **50**, 11062–11087.
155 Q.-L. Yang, X.-Y. Wang, J.-Y. Lu, L.-P. Zhang, P. Fang and T.-S. Mei, *J. Am. Chem. Soc.*, 2018, **140**, 11487–11494.
156 S. Kathiravan, S. Suriyanarayanan and I. A. Nicholls, *Org. Lett.*, 2019, **21**, 1968–1972.
157 C. Tian, U. Dhawa, A. Scheremetjew and L. Ackermann, *ACS Catal.*, 2019, **9**, 7690–7696.
158 S.-K. Zhang, R. C. Samanta, N. Sauermann and L. Ackermann, *Chem. – Eur. J.*, 2018, **24**, 19166–19170.
159 S. Enthaler and A. Company, *Chem. Soc. Rev.*, 2011, **40**, 4912–4924.
160 S. V. Ley and A. W. Thomas, *Angew. Chem., Int. Ed.*, 2003, **42**, 5400–5449.
161 L. McMurray, F. O'Hara and M. J. Gaunt, *Chem. Soc. Rev.*, 2011, **40**, 1885–1898.

162 L. Ackermann, *Org. Process Res. Dev.*, 2015, **19**, 260–269.
163 S.-K. Zhang, J. Struwe, L. Hu and L. Ackermann, *Angew. Chem., Int. Ed.*, 2020, **59**, 3178–3183.
164 R. Shang, L. Ilies and E. Nakamura, *Chem. Rev.*, 2017, **117**, 9086–9139.
165 G. Cera and L. Ackermann, *Top. Curr. Chem.*, 2016, **374**, 57.
166 C. Zhu, M. Stangier, J. C. A. Oliveira, L. Massignan and L. Ackermann, *Chem. – Eur. J.*, 2019, **25**, 16382–16389.
167 K. Tsuchida, T. Kochi and F. Kakiuchi, *Asian J. Org. Chem.*, 2013, **2**, 935–937.
168 K. Mitsudo, T. Kaide, E. Nakamoto, K. Yoshida and H. Tanaka, *J. Am. Chem. Soc.*, 2007, **129**, 2246–2247.